Author/s:
Guo, D;Westra, S;Maier, HR

Title:
Impact of evapotranspiration process representation on runoff projections from conceptual rainfall-runoff models

Date:
2017-01-01

Citation:
Guo, D., Westra, S. & Maier, H. R. (2017). Impact of evapotranspiration process representation on runoff projections from conceptual rainfall-runoff models. Water Resources Research, 53 (1), pp.435-454. https://doi.org/10.1002/2016WR019627.

Persistent Link:
https://hdl.handle.net/11343/292296

TITLE PAGE

Title: Impact of evapotranspiration process representation on runoff projections from conceptual rainfall-runoff models

Author names and affiliations: Danlu Guo[a]; Seth Westra[a]; Holger R. Maier[a].

[a] School of Civil, Environmental and Mining Engineering, the University of Adelaide, North Terrace, Adelaide SA 5005, Australia.

Corresponding author: Danlu.Guo@Adelaide.edu.au

Permanent address: School of Civil, Environmental and Mining Engineering, the University of Adelaide, North Terrace, Adelaide SA 5005, Australia.

Key Points:

1. Contrasting ET process representations can have substantial impact on runoff projections under a changing climate
2. Conceptual rainfall-runoff models can interact with potentially complex changes to PET, causing contrasting runoff projections
3. Comparing AET simulations with observations provides useful insights to evaluate the process representation within rainfall-runoff models

ABSTRACT

Conceptual rainfall-runoff models are commonly used to estimate potential changes in runoff due to climate change. The development of these models has generally focused on reproducing runoff characteristics, with less scrutiny on other important processes such as the conversion from potential evapotranspiration (PET) to actual evapotranspiration (AET). This study uses three conceptual rainfall-runoff models (GR4J, AWBM and IHACRES_CMD) and five catchments in climatologically different regions of Australia to explore the role of ET process representation on the sensitivity of runoff to plausible future changes in PET. The changes in PET were simulated using the Penman-Monteith model and by perturbing each of the driving variables (temperature, solar radiation, humidity and wind) separately. Surprisingly, the results showed the potential of a more than seven-fold difference in runoff sensitivity per unit change in annual average PET, depending on both the rainfall-runoff model and the climate variable used to perturb PET. These differences were largely due to different ways used to convert PET to AET in the conceptual rainfall-runoff models, with particular dependencies on the daily wet/dry status, as well as the seasonal variations in store levels. By comparing the temporal patterns in simulated AET with eddy-covariance-based observations at two of the study locations, we highlighted some unrealistic behaviour in the simulated AET from AWBM. Such process-based evaluations are useful for scrutinizing the representation of physical processes in alternative conceptual rainfall-runoff models, which can be particularly useful for selecting models for projecting runoff under a changing climate.

INDEX TERMS AND KEYWORDS

Keywords: evapotranspiration; climate impact assessment; GR4J; AWBM; IHACRES, conceptual rainfall-runoff model; AET simulation

1 INTRODUCTION

Climate change is expected to have significant implications on catchment-scale water resources, potentially affecting water security for municipal, agricultural, and industrial applications, environmental water quantity and quality, and flood hazard [*CSIRO and Bureau of Meteorology*, 2015; *Hauser et al.*, 2009; *IPCC*, 2014; *Turral et al.*, 2011]. To assess these implications, rainfall-runoff models are commonly used to translate projected changes in atmospheric variables derived from large-scale general circulation models into regional or local runoff [for examples see *Akhtar et al.*, 2008; *Chiew et al.*, 2009]. This information can then be used to assess catchment yield [e.g. *Haque et al.*, 2015], water quality [e.g. *Crossman et al.*, 2013], water supply security [e.g. *Christensen et al.*, 2004; *Paton et al.*, 2013; 2014] and flood risk [e.g. *Kay and Jones*, 2012], amongst other variables.

Although various rainfall-runoff model classes have been developed with different levels of physical realism [*Beven*, 2011], most climate impact studies are based on the outputs of one or several calibrated conceptual rainfall-runoff models [*Chiew et al.*, 2010; *Islam et al.*, 2014; *Najafi and Moradkhani*, 2015; *Vaze and Teng*, 2011]. The benefit of using conceptual rainfall-runoff models is that they are parsimonious and tend to perform well when calibrated to historical runoff data [*Perrin et al.*, 2003; *Wagener et al.*, 2003], particularly when compared to more complex physically-based and spatially distributed models, for which parameter estimation can be extremely challenging [*Beven*, 2001b; *Butts et al.*, 2004; *Goderniaux et al.*, 2009]. However, since the performance of these conceptual rainfall-runoff models is largely assessed on runoff, in many cases the underlying physical processes such as evapotranspiration fluxes, runoff generation mechanisms and so on can be poorly represented [*Li et al.*, 2015; *Seibert and McDonnell*, 2002; *Seibert et al.*, 2003], with parameters being 'falsely adjusted' to maximize runoff performance without considering the realism of the internal physical processes [*Andréassian et al.*, 2004; *Beven, 2001a; Clark et al., 2016; Ewen et al.*, 2006; *Minville et al.*, 2014] .

The surprisingly limited impact of physical process realism on the performance of conceptual rainfall-runoff models in simulating historical streamflow has been observed in multiple studies [*Brouyère et al.*, 2004; *Hartmann and Bárdossy*, 2005; *Kirchner*, 2006; *Vaze et al.*, 2010]. This result has also been found in the specific context of evapotranspiration (ET) process representation, and reasonable performance of conceptual models has been obtained with the use of simplified methods for estimating potential ET (PET) that do not realistically consider the dynamics in all its driving climate variables [*Oudin et al.*, 2005], or do not sufficiently represent the spatial and temporal variations in ET [*Andréassian et al.*, 2004*; Chapman, 2003*]. Furthermore, reasonable conceptual rainfall-runoff model performance has been observed even when the ET input contains systematic and/or random errors [*Oudin et al.*, 2006]. A potential reason for these findings is that the calibration process of conceptual models can 'compensate' for reasonable levels of differences in ET estimates without significant impact on model performance in simulating runoff [*Andréassian et al.*, 2004*; McMahon, 2015*]. However, although such calibrated conceptual models may perform well when applied under conditions similar to the period used for calibration, the extent to which they can be applied to climatologically different conditions is less clear [*Coron et al.*, 2012; *Klemeš*, 1986; *Wagener et al.*, 2003; *Westra et al.*, 2014], as in this context it becomes much more critical to ensure that the model 'gets the right answers for the right reasons' [*Kirchner*, 2006]. This is highlighted in a number of recent studies that found that although conceptual models with different structures can perform similarly when simulating historical runoff, they can produce very different estimates under a changing climate [*Bae et al.*, 2011; *Bastola et al.*, 2011; *Jiang et al.*, 2007; Mandoza et al., 2016; *Velázquez et al.*, 2013].

Although the above studies suggest potential limitations in the performance of conceptual rainfall-runoff models under future climate, the specific role of ET representation within these models on runoff projections has not been widely investigated. Changes to ET-related processes are likely to be particularly important to overall catchment response, as actual ET (AET) volumes exceed runoff volumes for the majority of catchments worldwide [*Dingman*, 2015]. Furthermore, the potential changes in the climatic variables that can influence ET (e.g. temperature, solar radiation, humidity and wind) [*IPCC*, 2014] suggest that changes to ET-related processes could be extremely complex, with changes not only at annual timescales but also in terms of the daily and seasonal distributions of ET [as illustrated in *Gong et al.*, 2006; *Huo et al.*, 2013; *Vicente-Serrano et al.*, 2014]. However, the extent to which these potentially complex changes to ET can interact with the structure of conceptual rainfall-runoff models remains unknown, with these changes usually represented using seasonal or annual ET change factors in many climate impact studies [e.g. *Chiew et al., 2009; New et al., 2007; Teng et al., 2012*].

The focus of this study is therefore to assess the impact of alternative ET process representations within conceptual rainfall-runoff models on runoff projections under perturbed climate conditions. This is achieved by focusing specifically on the following research questions:

1. To what extent can ET process representations within conceptual rainfall-runoff models impact runoff projections under plausible changes in the climate drivers of ET?
2. How do alternative conceptual rainfall-runoff model structures interact with the potentially complex changes to PET to produce projections of runoff and AET?
3. Is it possible to use AET observations to constrain which ET process representations within conceptual rainfall-runoff models are more realistic?

The above research questions were addressed with five case study locations from distinct climatic regions within Australia. Three lumped conceptual rainfall-runoff models—GR4J, AWBM and IHACRES_CMD—were used to represent contrasting ET process representations, and thus to illustrate how potential changes in PET can propagate differently to runoff projections. PET was required as an input to all three rainfall-runoff models, and was estimated using the Penman-Monteith method. This method is considered to be the most comprehensive physically based PET model and is thus widely used for rainfall-runoff modelling and climate impact assessments [e.g. *Arnell*, 2004; *Gosling et al.*, 2011; *Kay et al.*, 2009]. Use of the Penman-Monteith method enables an assessment of the effect of perturbing each of the driving climatic variables of PET (i.e. temperature, solar radiation, wind and humidity), and can provide information not only on annual average changes, but also on sub-annual (e.g. daily and seasonal) variations in PET sensitivity.

The remainder of this paper is structured as follows. The data used to address the three research questions are provided in the next section, together with an overview of the Penman-Monteith model and the three conceptual rainfall-runoff models. This is followed by a description of the methods employed to address each research question in Section 3. The results and their implications are discussed in Section 4, and a summary and conclusions are given in Section 5.

2 DATA AND MODELS

2.1 Data

Figure 1 shows the names and locations of the five case study catchments, which are situated in climatologically different regions in Australia, as defined in the Australian Köppen climate classifications of *Stern et al.* [2000]. As mentioned in the Introduction, three lumped conceptual rainfall-runoff models were used in this study, which required historical data for calibration. These data include catchment-average rainfall, PET and runoff at each location. The PET input data to these models were estimated using the Penman-Monteith model, which required data on temperature, relative humidity, solar radiation and wind speed.

Figure 1: Locations for rain gauges, catchment outlets and weather stations from which data were obtained for calibration of rainfall-runoff models at the five case study catchments. The locations of two flux towers to obtain data for model evaluation at Alice Springs and Wagga Wagga are also shown. Coloring relates to Köppen climate classifications from *Stern et al.* [2000].

The source of each data variable is summarized below, with further details given in Table S1 of the supplementary information:

1. **Catchment runoff (ML/day)**: Daily runoff data were obtained from the gauging stations at the outlet of each catchment.
2. **Catchment-average rainfall (mm/day)**: In order to represent the catchment-average rainfall, daily rainfall data were obtained from a rain gauge within each of the four smaller catchments (Scott Creek, Black River, Elizabeth River and Adelong Creek). For the largest catchment (Hugh River), data from three rainfall gauges within the catchment were spatially averaged using the Thiessen polygon method.
3. **Daily maximum and minimum temperature (T_{max} and T_{min} in °C), maximum and minimum relative humidity (RH_{max} and RH_{min} in %) and wind speed (u_z in m/s):** Due to the limited availability of high-quality climate observations, data for each of these variables were obtained from a weather station outside but nearby each catchment.
4. **Daily solar radiation (R_s in MJ/(m^2.day)):** Daily solar radiation was calculated from daily sunshine hour data (n in hrs) obtained from each weather station, using the Ångström-Prescott equation [*McMahon et al.*, 2013] with constants for each location provided in *Chiew and McMahon* [1991].

Data for each variable were obtained for a consistent period from 1 January 1995 to 31 December 2003 at each location, with key statistics presented in Table 1. As can be seen, there are large differences in the average values of each variable, highlighting the potentially significant differences in dominant physical processes for ET and runoff production across these catchments. A quantity particularly relevant to ET processes is the long-term averaged ratio of PET to precipitation (PET/P), which describes whether a catchment is water-limited (PET/P >1) or energy-limited (PET/P < 1). The range of PET/P values indicates substantial variations in the water availability conditions at the five study sites.

Table 1: Average climate conditions at the five case study locations between 01/01/1995 and 31/12/2003.

To determine the relative realism of different ET process representations, actual measurements of AET were used to benchmark the simulated AET from the three rainfall-runoff models. A challenge, however, is the limited availability of AET data for Australia. Lysimeter measurements are currently considered as the most accurate source of AET observations [*Seneviratne et al.*, 2012; *Wang and Dickinson*, 2012]; however, these data are most commonly available in irrigated regions [e.g. *Bethune et al.*; *Northey et al.*, 2006; *Zhang et al.*, 1999], with measurements from natural catchments being very scarce. The MODIS Land Product (http://daac.ornl.gov/MODIS/modis.shtml) also provides estimates of AET based on remotely sensed observations [*Cleugh et al.*, 2007; *Mu et al.*, 2011] with a much wider spatial coverage; however, the AET data are only available on an 8-day interval.

The above constraints led us to select eddy covariance (EC)-based AET measurements, which are available through the OzFlux [*TERN*, 2012] network at 30 active sites across Australia (see: http://www.ozflux.org.au/). For our purpose of evaluating alternative ET representations, the AET observations should be obtained from nearby our case study catchments, as well as spanning a sufficient continuous time period. As a result of these constraints, only two OzFlux sites were selected, namely Alice Springs Mulga, which is close to the Hugh River catchment, and Tumbarumba, which is close to the Adelong Creek catchment [*Cleverly, 2011; vanGorsel, 2013*]. Based on the EC data availability, the comparison between modelled and observed AET used a study period of between 3 September 2010 and 31 July 2014 for both catchments. The corresponding climatic and rainfall data within this period were also obtained from both flux sites to ensure internal consistency in the rainfall-runoff models.

2.2 Models

2.2.1 Penman-Monteith PET model

The Penman-Monteith model was adopted throughout this study, which combines the energy balance and mass transfer components of ET. To minimize the potential confounding effects of differences in vegetated surface, the evaporative surface was assumed to be reference crop for all study sites, for which the FAO-56 version of the Penman-Monteith model [*Allen et al.*, 1998] was used. The FAO-56 Penman-Monteith model was implemented using the R package 'Evapotranspiration' (http://cran.r-project.org/web/packages/Evapotranspiration/index.html) [*Guo et al.*, 2016].

2.2.2 Three conceptual rainfall-runoff models

Contrasting ET process representations were considered by using three rainfall-runoff models (GR4J, AWBM and IHACRES_CMD), which all run on a daily time-step. The three models are all lumped conceptual models, although with very different soil moisture accounting (SMA) routines, which can affect the partitioning of precipitation into AET and runoff. To isolate the effect of different conceptual ET representations in the three models, the groundwater exchange was set to zero for each model. Furthermore, the routing components for all models were constrained to the GR4J routing model, so that differences between models can be attributed specifically to the SMA routines.

The first model, GR4J [*Perrin et al.*, 2003], is a conceptual hydrologic model based on a SMA production store and an excess-rainfall routing store. The model requires two input variables, PET and precipitation (P). Interception is treated as a store with zero capacity, so that each day can be either 'wet' (P > PET), which produces a net precipitation P_n = P-PET, or 'dry' (P < PET) with a net evapotranspiration E_n = PET-P. For wet days a portion of the net precipitation P_n fills the production store. This portion is termed P_s and is a function of both P_n and the store level S relative to its capacity defined by parameter x_1. Runoff is produced from the total water available for routing, P_r, which is generated by the remaining net precipitation (P_n-P_s). The conversion of PET to AET from the production store is illustrated in Figure 2a, which relies on the wet/dry status of a day. For wet days, AET is set to be equal to PET. For dry days, AET is modelled as the sum of the precipitation and the evapotranspiration from store E_s, which is modelled as a fraction of the net evapotranspiration E_n depending on the water level in the production store S relative to x_1. Consequently, AET is always less than PET on dry days.

The schematic of AWBM is shown in Figure 2b. In contrast to GR4J, the production store in AWBM [*Boughton*, 2004] is represented by three individual stores (termed S_1, S_2 and S_3) with different capacities, and each store occupies a fixed fraction of the total catchment area, with the default values of 0.134, 0.433 and 0.433 used in this study. For each day precipitation P is added directly to each store without explicit consideration of interception. For each non-empty store, available runoff P_r is produced from any excess when the store is full, while evapotranspiration from the store, E_s, always equals PET until the store is completely empty [*Boughton*, 2009]. Therefore, the overall AET, as the sum of E_s from all three stores, equals different proportions of PET, depending on which stores contain water. Specifically, the AET as a proportion of PET can be one of: 0 (when all three stores are empty), 0.134 (when both of S_2 and S_3 are empty), 0.433 (when both of S_1 and S_2 or both of S_1 and S_3 are empty), 0.567 (when only one of S_2 or S_3 is empty), 0.866 (when only S_1 is empty), or 1 (when all stores are non-empty). The level for each store S_i ($i = 1, 2, 3$), after accounting for P, PET and P_r from the specific store, equals S_i + P – PET – $P_{r,\, i}$. Therefore, on days with P – PET > 0, all stores are filled up (i.e. with increase in store levels), resulting in the overall AET = PET; when P – PET < 0, AET is always less than PET as determined by number of empty stores.

In IHACRES_CMD [*Croke and Jakeman*, 2004], the level of the store is represented by the catchment moisture deficit (CMD), which is the difference between the current level and the saturation level of the store. The schematic of the model is shown in Figure 2c. For each day, all precipitation P directly fills the store without explicit consideration of interception. The total water available for routing, P_r, is a proportion of P, which decreases with increasing ratio of *CMD* relative to a flow-production threshold parameter *d*. AET is taken directly from the store (i.e. E_s = AET), which is estimated as a fraction of PET depending on whether *CMD* exceeds a threshold parameter *g*. When *CMD* > *g*, the fraction of AET to PET is always less than one, which decreases with increasing ratio of *CMD* to *g*, and approaches an asymptote of 0. In contrast, when *CMD* < *g*, AET = PET. Therefore, the conversion from PET to AET is independent of direct input of P, other than through its effect on changing the store levels.

Figure 2: SMA routines in: a) GR4J; b) AWBM; and c) IHACRES_CMD (adapted from *Perrin et al.* [2005], *Boughton* [2004], *Croke and Jakeman* [2004] respectively). The red arrows represent dry days and the blue arrows represent wet days in each model.

The above rainfall-runoff models therefore provide examples of three contrasting methods of converting PET input data to AET: GR4J explicitly considers both the impact from store levels and the wet/dry status of a day, defined by individual rainfall events; AWBM simulates AET mostly as a function of rainfall which determines the wet/dry status, while the impact of instantaneous store levels is largely eliminated by the use of step functions to relate AET with the emptiness of each store; finally, IHACRES_CMD simulates AET as a function of only the store level and thus is relatively independent of rainfall for that day.

To simulate runoff, the PET data estimated for each case study were used as input to all three SMA models linked with the GR4J-routing model (implemented using the R package 'hydromad', available at: http://hydromad.catchment.org/ [*Andrews and Guillaume*, 2013]). For each case study, the three models were calibrated to the first six years of historical runoff data (from 1 January 1995 to 31 December 2000) at a daily time-scale, with the first year (1995) used as a warm-up period. The remaining three years of data (from 1 January 2001 to

31 December 2003) were used for validation. The objective function for calibration was the Nash-Sutcliffe coefficient of efficiency (NSE), which has been used widely in rainfall-runoff modelling. In addition, the relative bias was also calculated to assess the bias in modelled runoff relative to observations.

The calibration and validation results are shown in Table 3. For each model, the calibration and validation performance varies by catchment, and the validation performance is on average slightly lower than the calibration performance. For each catchment, the values of each performance metric are generally similar across the three rainfall runoff models, although GR4J on average has the best performance and AWBM has the worst performance for the case study catchments.

Table 3: NSE for calibration and validation for the GR4J, AWBM and IHACRES_CMD models at the five case study sites, with relative bias shown in brackets.

3 METHOD

A schematic of the methodology is presented in Figure 3. The approach to addressing the three research questions described in the Introduction is detailed in Sections 3.1 to 3.3, respectively.

Figure 3: Schematic of methodology used to address the research questions posed in the Introduction.

3.1 Impact of ET process representations on runoff projections

To assess the impact of different ET process representations within conceptual rainfall-runoff models, we explored the sensitivity of both PET and runoff to changes in four climate variables related to PET, with differences in the ratio of sensitivity values between PET and runoff providing an indicator of the importance of ET process representation. The sensitivity curve method was employed to achieve this, as it has been widely applied in previous PET sensitivity studies due to its computational convenience and ease of interpretation [*Goyal*, 2004; *McKenney and Rosenberg*, 1993; *Vicente-Serrano et al.*, 2014].

As required by the sensitivity curve method, perturbations were made to the four climatic variables which influence PET, namely temperature (T), relative humidity (RH), solar radiation (R_s) and wind speed (u_z), at each of the five study sites. This process yields multiple sets of perturbed climate data, each obtained by perturbing one climate variable while keeping the others unchanged. It is worth noting that by perturbing each input variable independently, the sensitivity curve method does not take into account the potential joint-variations among the input variables due to correlations. However, according to a previous global sensitivity study across multiple locations in Australia, PET generally showed little sensitivity to these joint-variations among T, RH, R_s and u_z [*Guo et al., 2016, in review*], so that it is reasonable to assume that this one-at-a-time climate perturbation is capable of capturing the majority of potential changes in PET due to the four climatic variables.

The bounds for perturbing each variable were selected to be slightly wider than the ranges of the projected changes in these variables by 2100 for Australia [*Stocker et al.*, 2013] to encompass a comprehensive range of plausible future climate change scenarios (Table 2).

Table 2: Plausible perturbation ranges for each climate variable relative to their historical levels.

For each climate variable, the perturbation levels relative to its historical baseline consisted of four equidistant levels within the above-mentioned plausible ranges (i.e. +2, +4, +6 and +8°C for *T*, -10%, -5%, +5% and +10% for *RH* and R_s, and -20%, -10%, +10% and +20% for u_z), with each perturbation level being applied as a factor to the entire time series of the corresponding daily historical data. For *T* and *RH*, the Penman-Monteith model requires both the daily minimum and maximum values as input; therefore, the daily time-series of each pair of *T* and *RH* variables was considered jointly and thus perturbed by the same amount for each day. Since all perturbations for *T* were additive, whereas perturbations for R_s, *RH* and u_z were percentage changes, positive values of these variables were maintained during the perturbation. The perturbed *RH* data were also capped at 100% to avoid obtaining physically unrealistic humidity values. The sensitivity of PET and runoff to different levels of perturbation in each of *T*, *RH*, R_s and u_z were then represented as the relative changes to their corresponding baseline historical data, as used in model calibration.

To compare the PET sensitivity with the runoff sensitivity from the three rainfall-runoff models, the ratio of the percentage change in annual average runoff for each percentage change in annual average PET—referred to as the runoff 'elasticity' to changes in PET [*Chiew*, 2006]—was also estimated.

3.2 The role of rainfall-runoff model structure on sensitivity to PET

The focus of this section is to better understand the effect of rainfall-runoff model structure on the sensitivity of runoff to changes in PET. As discussed in Section 2.2.2, the key structural differences of three rainfall-runoff models in the context of translating PET to AET and runoff are their manner of: (a) converting PET to AET on wet days and dry days; and (b) relating AET to the level of the soil moisture store(s). Therefore, to understand the causes of the impact of ET process representations on runoff projections, we investigated the impact of the following factors on the sensitivity of simulated runoff to PET:

1. Wet-day and dry-day patterns, to assess how rainfall-runoff models handle conversion from PET to AET on wet and dry days. Although the three rainfall-runoff models use different definitions of wet and dry days to determine how much of PET is converted to AET, for consistency we used a single definition of a wet day as one with rainfall greater than 1 mm for all models. The conversion from PET to AET was represented by the AET:PET ratio, which should be between 0 and 1 by definition. We compared the wet-/dry-day distributions of: (a) the daily PET responses to perturbations in each climate variable; and (b) the daily AET:PET ratios simulated from each rainfall-runoff model. We also investigated whether there were interactions between them that can lead to different AET estimates for the same change in average PET.
2. Seasonal patterns, to assess how rainfall-runoff models relate AET to temporal variations in storage. Depending on the catchment, there is evidence that the production store can vary significantly by season (for example, see *Westra et al.* [2014]). Therefore, we investigated the role of seasonality in storage on the simulated AET from rainfall-runoff models. We also investigated whether the responses of PET

to each perturbed climate variable can vary seasonally and thus act synergistically or antagonistically to produce different AET simulated for the same total change in annual average PET. This was achieved by investigating the seasonal variations in: (a) the daily response of PET to perturbations in each individual climate variable; (b) the daily AET:PET ratios simulated in the three rainfall-runoff models; and (c) the daily storage levels simulated in the three rainfall-runoff models.

To provide a common basis for comparison, all the sensitivity results in this section were presented per 1% change in PET.

3.3 Relative realism of alternative ET process representations within conceptual rainfall-runoff models

To evaluate the relative realism of ET process representations within the three conceptual rainfall-runoff models, the AET simulated with the three models were compared with EC measurements of AET at Alice Springs and Wagga Wagga, as these were the only sites at which measured AET data were available. As a result of limitations in AET measurements at these sites (as discussed in Section 2.1), a qualitative approach was adopted for the comparison, in which the times-series of observed and simulated AET were visually compared to evaluate each model's ability to represent the temporal variation of ET processes.

4 RESULTS AND DISCUSSION

4.1 Impact of ET process representations on runoff projections

The sensitivity of PET and runoff to changes in each climate variable are shown in Figure 4, with each panel representing the sensitivity to a different climate variable (see Figures S1 and S2 in the supplementary material for individual plots of PET and runoff sensitivity). The results show a large range of sensitivity values depending on (a) the perturbed climate variable, (b) the rainfall-runoff model and (c) the location. For example, PET is generally more sensitive to perturbations in T, with an 8°C increase in T leading to between a 20% and 32% increase in average PET depending on location (Figure 4a). RH shows a negative relationship with PET, with a 10% increase in average RH leading to between a 2% and 13% decrease in average PET (Figure 4b). Sensitivity to R_s and u_z are consistently much smaller, with the increase in PET being between 3% and 5% for a 10% increase in average R_s (Figure 4c), and between 3% and 6% for a 20% increase in average u_z (Figure 4d).

Figure 4: Sensitivity of PET and runoff to the four perturbed climate variables at the five study sites. The sensitivities for PET are represented by solid lines while for runoff dashed lines are used.

Also apparent from Figure 4 is that for a fixed climate perturbation, the runoff sensitivity always has an opposite sign to that of PET. However, the relative order of impact that the four climate variables have on runoff is consistent with that for PET. In particular, runoff generally shows a higher sensitivity to perturbations in T, for which an 8°C increase can cause between a 7% and 31% decrease in runoff depending on the location and rainfall-runoff model used (Figure 4a). RH also shows substantial sensitivity, leading to up to between a 3% and 10% increase in runoff for a 10% increase in RH (Figure 4b). R_s and u_z show much smaller impacts, with a 10% increase in R_s causing between a 1% and 4% decrease in runoff (Figure 4c), while a 20% increase in u_z can cause between a 1% and 8% decrease in runoff

(Figure 4d). For both PET and runoff, the relationship between sensitivity values and perturbations in each climate variable are highly linear, suggesting that the results can be represented per unit change for both PET and runoff.

To assess the specific role of rainfall-runoff model choice on the sensitivity values in Figure 4, the runoff elasticity (i.e. the percentage change in annual average runoff for each percentage change in annual average PET) simulated from three rainfall-runoff models is plotted for each study site in Figure 5. For the two most humid locations (Darwin and Burnie, which have the lowest long-term PET/P ratios as shown in Table 1), the elasticity values do not vary much across rainfall-runoff models and climate variables—this will be discussed further in Section 4.3.

Figure 5: Runoff elasticity for different climate variables for each study site, as simulated from three rainfall-runoff models

For the remaining locations (i.e. Adelaide, Alice Springs and Wagga Wagga), the choice of both the rainfall-runoff model and the climate variable being perturbed makes a substantial difference to the runoff elasticity. Although all models suggest that runoff shows higher elasticity when perturbing *RH* rather than other climate variables, GR4J and AWBM consistently show much greater elasticity due to *RH*, compared to IHACRES_CMD. Focusing on Alice Springs, GR4J suggests that for each 1% change in PET, perturbing *RH* leads to the greatest change in runoff of 1.5%, whereas perturbing u_z leads to the smallest runoff change of only 0.2%. This is equivalent to an over seven-fold difference in runoff elasticity attributable solely to perturbing different climate variables. A similar magnitude of difference in runoff elasticity is observed for AWBM. In contrast, IHACRES_CMD suggests that the runoff elasticity for perturbing all four climate variables is below 1%. This is quite surprising, as these conceptual rainfall-runoff models do not directly use the four climate variables as inputs, but instead use the PET estimated with the Penman-Monteith model. Consequently, the fact that the variation of runoff responses depends on the climate variable being perturbed clearly illustrates the impact of ET process representations within individual rainfall-runoff models on propagating climate change signals to projected runoff.

To better understand these findings, in the next section we investigate the effect of rainfall-runoff model structure on the varying elasticity values shown above.

4.2 The role of rainfall-runoff model structure on sensitivity to PET

In the previous section, it was shown that the elasticity of runoff varied significantly depending on the variables used to perturb PET. Given that the results in Figure 5 are presented per unit change in annual average PET, it is anticipated that differences in elasticity values must be due to sub-annual variations that are different depending on the perturbing variable.

In this section we therefore assess the role of sub-annual variations in PET on runoff sensitivity, with a focus on daily and seasonal variations. For illustration purposes, we use the results from Alice Springs, which exhibited the largest differences in runoff elasticity among the climate variables (Figure 5), and is thus expected to illustrate the most significant impact of ET process representations. Analyses from other sites generally led to conclusions that are consistent with those from Alice Springs, and are available in Figure S6 to Figure S17 in the supplementary material.

4.2.1 Interactions between PET sensitivity and AET simulated for wet and dry days

Figure 6a shows the wet/dry-day distribution of PET changes for a 1% change in annual average PET. Note that the same distribution of PET responses applies to GR4J, AWBM and IHACRES_CMD, since no rainfall-runoff modelling is yet involved. The figure indicates that for a fixed average change in PET, there are significant differences in the change for wet and dry days. Among all climate variables, *RH* causes the greatest difference in average dry-day and wet-day sensitivities of PET (0.743% and 3.04%, respectively). T and R_s also show lower sensitivity for dry days compared to wet days, but the differences are much smaller compared to those for *RH* (with the two sensitivities becoming 0.989% and 1.01% for T, and are 0.917% and 1.27% for R_s, respectively). In contrast, u_z leads to higher sensitivities on dry days compared to wet days (with averages of 1.06% and 0.567%, respectively).

Figure 6: (a) Distribution of PET changes on wet and dry days, in response to perturbations in each climate variable (in each vertical panel) that result in an annual average PET change of 1% (indicated by the red dashed line), where a red dot represents the mean for each group; (b) all daily PET changes that lead to a 1% change in annual average PET from perturbing *RH*, against different baseline levels of *RH* for wet and dry days; and (c) AET:PET ratios on wet and dry days, simulated from AWBM, GR4J and IHACRES_CMD (in each vertical panel).

The substantially higher PET sensitivity to *RH* can be explained with the aid of Figure 6b, where all daily PET changes that led to a 1% change in annual average PET from perturbing

RH (as the second panel in Figure 6a) are plotted against the corresponding baseline daily *RH*. The figure shows that: (a) wet days are typically associated with high baseline *RH*; (b) these high-*RH* wet days generally lead to greater change in PET. These illustrate that part of the higher PET sensitivity on wet days can be the result of using multiplicative perturbation for *RH*, as the average *RH* on wet days is around 1.5 times of that for dry-day *RH*, leading to greater perturbation of *RH* on wet days than on dry days with any scaling factor. However, the use of a multiplicative perturbation method does not fully explain the four-fold difference in wet-/dry-day PET sensitivity in Figure 6a, which suggests that the structure of the Penman-Monteith model also contributes to greater PET changes during wet days compared to dry days.

Having shown that the PET sensitivity differs from wet to dry days depending on the perturbing climate variable, we now investigate how PET is converted to AET differently on wet and dry days via different rainfall-runoff models. Figure 6c presents the distribution of daily AET:PET ratios on wet and dry days, simulated from the three rainfall-runoff models. All three models illustrate higher ratios of AET:PET during wet days compared to dry days, with GR4J and AWBM showing greater differences than IHACRES_CMD. This is because GR4J and AWBM both determine if AET = PET by checking if P – PET > 0, which produces a peak ratio of one for most wet days, while those below one correspond to days with P > 1 mm, but still not yet satisfying P – PET > 0. In contrast, IHACRES_CMD only uses store levels to determine AET, which is therefore largely independent of individual rainfall events, so that it does not lead to substantially higher AET on wet days. For dry days, the AET:PET ratios from GR4J and IHACRES_CMD show similar distributions, in contrast to those from

AWBM. Although most dry-day ratios from GR4J and IHACRES_CMD are around zero, they can vary substantially with values spanning the entire range from zero to one, highlighting the direct impact of instantaneous store levels on AET in both models. In AWBM, this ratio is mostly zero with only a few anomalies, corresponding to dry days that have small rainfall amounts ($0 < P < 1$ mm), but still with water in some or all of the stores, leading to overall AET at discrete ratios of PET (i.e. 0, 0.433, 0.866 and 1).

Connecting these results with those in Figure 5, it is clear that for a fixed positive average change in PET, a greater decrease in runoff would be expected to occur for variables that cause the greatest change of PET during wet days, as a larger percentage of PET would be 'lost' to AET during wet days in both GR4J and AWBM. Based on this finding, one would expect the highest runoff elasticity for both models for *RH*, followed by R_s, T and finally u_z. This is exactly the same order as was identified for Alice Springs in Figure 5.

4.2.2 Interactions between seasonal variations in PET sensitivity, simulated AET and storage

We now consider the role of seasonal patterns in the changes in PET as a result of perturbing each climate variable, and how they interact with simulated AET and storage. Figure 7a shows the seasonal distributions of the daily PET responses to perturbations in each climate variable that result in a 1% average change in PET at Alice Springs for the year 2000. The figure highlights substantial differences in the temporal distribution of PET responses, depending on the climate variable perturbed. For perturbations in *RH*, PET responses display high temporal variability: two clear peak periods are shown around February and May with the highest PET response exceeding 15 times average levels, while from July to October most responses are close to zero. In contrast, the variability in PET responses to the perturbations in T, R_s and u_z are much smaller and close to 1% for the entire year.

Figure 7: Seasonality of a) daily PET responses to perturbations in each climate variable that result in an average PET change of 1% (black dashed line); b) AET:PET ratios for wet and dry days from GR4J, AWBM and IHACRES_CMD; and c) levels of production stores from GR4J, AWBM (with dashed lines indicating store capacities) and IHACRES_CMD (as CMD levels). All results are from Alice Springs for the year 2000.

Having shown the different seasonal variations in the PET sensitivity depending on the perturbing climate variable, we now investigate the seasonal patterns in the conversion from PET to AET within the three rainfall-runoff models. The simulated daily time-series of AET:PET ratios from the three models are shown in Figure 7b for Alice Springs for the year 2000.

Considering firstly the results from January to October, all models suggest two periods with peak AET:PET ratios occurring around February and May, respectively, which correspond to the simulated store levels from all models (Figure 7c), which also show two consistent peak periods. Following the peak periods, the models show contrasting temporal patterns in both AET and storage: from both GR4J and IHACRES_CMD, the AET:PET ratios show a smooth "recession period" from one to close to zero, while the store drains gradually at the same time. This is because both models limit the rate of AET when store levels decrease. In contrast, the role of the store level in simulated AET is less obvious for AWBM, as the AET:PET ratios drop in a 'stepwise' fashion (from 1 to levels of 0.866, 0.433 and then 0) following each peak period, corresponding to times when different stores become empty (as detailed in Section 2.2.2). In addition, compared to GR4J and IHACRES_CMD, the stores simulated in AWBM drain at a more constant rate (for example before April), because this model forces each store to keep evaporating at the rate of PET until empty.

Interestingly, after October, GR4J and AWBM both show instantaneous high AET:PET ratios on wet days, but returning to lower values once the rainfall ceases. This indicates the impact of individual rainfall events, which is independent of that of storage, since peak ratios can occur even when storage levels are consistently low. Such impact is not visible from IHACRES_CMD as it does not relate AET simulation to individual rainfall.

From these results, all three models show a fuller storage around both February and May. Since all models relate AET simulation to storage, a greater amount of PET is also converted to AET during this period, with associated implications on runoff volume. As these periods also correspond to when *RH* can cause the greatest changes in PET, we can expect that for a fixed positive average change in PET, perturbations in *RH* can lead to greater decreases in runoff from all three models. This, again, is consistent with the higher sensitivity of runoff to *RH* shown from all three models in Figure 5.

Combining results from Sections 4.2.1 and 4.2.2, we can see that:

1. PET shows substantially higher sensitivity to *RH* during wet days and around February and May;
2. Both GR4J and AWBM explicitly relate AET simulation to daily wet/dry status, leading to higher impact of changing PET on AET during wet days; and
3. All three models relate AET simulation to catchment storage, leading to higher impact of changing PET on AET when stores are fuller around February and May.

Relating the above results to observations for Alice Springs in Figure 5, it is clear that the higher elasticity values for *RH* compared to the other variables shown in all three models are likely to be attributable to these models having a higher contrast in the AET:PET ratios across different seasons where store levels vary substantially (Figure 7). Furthermore, the reason that GR4J and AWBM show even higher sensitivity to *RH* can be that these models having higher contrast in AET:PET ratios between wet day dry days across wet and dry days, which are associated with contrasting levels of *RH* (Figure 6).

In summary, in this section we show that there are clear daily and seasonal variations in the sensitivity of PET depending on which climate variable is perturbed. This can then interact with the way PET is converted to AET in the three models, which depends on whether a day is dry or wet, as well as the temporal variation in the production store. The interaction between these two mechanisms can lead to large variability in runoff sensitivity to different perturbing climate variables, even for the same change in annual average PET.

4.3 Relative realism of alternative ET process representations within conceptual rainfall-runoff models

Given the importance of rainfall-runoff model process representation in determining how much AET is converted from PET, we now investigate model realism by comparing observed time-series of AET with simulated AET from the three conceptual rainfall-runoff models at Alice Springs and Wagga Wagga (Figure 8).

For Alice Springs, the differences between model simulated AET clearly illustrate their contrasting ET process representations. GR4J illustrates both the effect of individual rainfall events, as well as change in store levels, with simulated AET peaking on individual wet days and gradually decreasing on the dry days after, which indicates drops in store levels. In AWBM, the effect of individual rainfall is also illustrated by the peak AET on wet days; however, the influence of retreating storage is not shown in AWBM, with AET either remaining at or near its peak value, or dropping suddenly to zero. This instantaneous drop is due to the 'discrete' function that AWBM uses to represent the relationship between AET and storage (as discussed in Section 2.2.2). In contrast to GR4J and AWBM, the simulated AET from IHACRES_CMD is not sensitive to individual rainfall events, as the occurrence of peak AET is not associated with wet days. This is because AET is simulated purely as a function of the moisture content in the store. In general, GR4J and IHACRES_CMD better resemble the temporal variation in the observed AET in Alice Spring, which indicates that the change in store levels is likely to be a key controlling mechanism for ET processes in this catchment.

Figure 8: Comparison of the observed and simulated time-series of AET from GR4J, AWBM and IHACRES_CMD, at a) Alice Springs; and b) Wagga Wagga.

In contrast to Alice Springs, all three models show reasonable performance in producing the temporal patterns in the observed AET at Wagga Wagga, with only slight differences across models suggesting a lower impact of ET process representation. As an exception, at the start of 2013 and 2014, AWBM shows zero-AET periods, which are clearly different from observations. As illustrated in Figure 7, these periods correspond to times when all storages are empty, as a result of AWBM keeping each store evaporating at the PET rate (i.e. AET=PET).

The comparisons of AET simulation at the two study sites indicate that the impact of ET process representations is likely to be greater for drier catchments such as Alice Springs, where stores vary substantially on a seasonal basis, and experience frequent draining and rapid changes of levels in response to rainfall. In contrast, Wagga Wagga is a somewhat more humid catchment with lower seasonal variability (although still water limited, see Table 1). As such, it generally has fuller storage levels, which neither drain out completely nor rise rapidly with individual rainfall events. Under this condition, the simulated AET is likely to be less sensitive to different ways of defining the relationships between the AET:PET ratio and the storage level (e.g. GR4J and AWBM). Furthermore, with the consistently fuller stores leading to higher AET overall, the impact of different ET representations across dry/wet status (e.g. GR4J and IHACRES_CMD) are likely to be limited. Therefore, model choice is likely to have less impact on ET simulations for catchments with relatively stable store levels. This can also be a possible explanation of the observations in Section 4.1, where humid locations, such as Darwin and Burnie, show fewer differences in runoff sensitivity to different climate variables across the three rainfall-runoff models.

It should be noted that although the EC-based AET measurements were used as a benchmark for the simulated AET from the three rainfall-runoff models, the comparison should be interpreted qualitatively rather than quantitatively, due to several limitations associated with the available data. In particular, both catchments used for this comparison were assumed to be covered with reference crop when estimating catchment PET for simulating AET (Section 2.2.1). However, the EC measurements were obtained from flux towers within tall canopy (Mulga woodland for Alice Springs and Eucalyptus forest for Wagga Wagga), which are likely to be valid only for a small region for the specific type of canopy around each flux tower, since EC measurements usually only cover spatial scales of hundreds of meters. This inconsistency can contribute to differences between the simulated and observed catchment AET. Furthermore, a number of studies have reported biases in AET measured by the EC method due to the failure to close the energy balance [e.g. *Wang and Dickinson*, 2012; *Wilson et al.*, 2001]. These biases appear to be particularly prominent for days with high relative humidity and wind [*Ibrom et al.*, 2007], as well as during turbulent conditions at night or when precipitation or dew obscured the sensors [*Meiresonne et al.*, 2003; *Meyer et al.*, 2015; *Wilson et al.*, 2001].

Despite the abovementioned limitations, the ET observations from the two sites illustrate contrasting temporal variations related to rainfall events and store levels, which can be explained by the unique characteristic of each catchment. Therefore, it is likely that these patterns shown in the data may nevertheless be useful to scrutinize rainfall-runoff models and assess which models simulate ET processes more realistically. Furthermore, the results also highlight potential opportunities for more detailed process-based evaluation of rainfall-runoff models where data are available, which can provide valuable insights to support rainfall-runoff model selection complementary to the use of conventional runoff-centered performance assessment (e.g. calibration metrics in Table 2). These process-focused assessments are particularly important when evaluating the suitability of models for simulating catchment behavior under changed conditions, where the differences in the runoff projections from alternative rainfall-runoff models are likely to be greatest.

5 SUMMARY AND CONCLUSIONS

In this study, we:

1. Assessed the impact of ET process representations within conceptual rainfall-runoff models on runoff projections under plausible changes in the climate drivers of ET;
2. Explored the interaction between conceptual rainfall-runoff model structure and the complex sub-annual changes in PET, and how this influences projections of runoff and AET; and
3. Evaluated the relative realism of alternative ET process representations within three conceptual rainfall-runoff models using AET observations.

We investigated five study sites across Australia with contrasting hydro-climatic conditions, at which the baseline PET was simulated using the Penman-Monteith model. Perturbation of PET was achieved by first perturbing the historical data of four climatic drivers of ET, namely temperature (T), relative humidity (RH), solar radiation (R_s) and wind (u_z), within plausible ranges of their future changes, and then estimating the corresponding PET with the Penman-Monteith model. The baseline and perturbed PET time series formed inputs to three structurally different conceptual rainfall-runoff models (GR4J, AWBM and IHACRES_CMD), which were calibrated to historical runoff data at the five study sites. The calibrated rainfall-runoff models were used to simulate the baseline and perturbed runoff, and then to estimate runoff sensitivity to climate perturbations.

Our results illustrate that different ET process representations in conceptual rainfall-runoff models can have substantial impacts on the sensitivity of runoff projection under a changing climate. Specifically, it is possible to have an over seven-fold difference in runoff elasticity due to rainfall-runoff model choice and the climate variable that is perturbed. The significant differences in runoff elasticity were attributed to the different conceptualizations used to convert PET to AET on wet and dry days in the three conceptual rainfall-runoff models, as well as the contrasting relationships defined between AET and store levels.

Using eddy-covariance-based observations of AET, we also compared and evaluated the ET process representations within the three conceptual rainfall-runoff models at Alice Springs and Wagga Wagga. Results suggest that alternative ET process representations are likely to have a greater impact on drier catchments consisting of highly variable store levels, such as

Alice Springs. As highlighted with the results from Alice Springs, AWBM poorly simulated the variations in observed AET, whereas GR4J and IHACRES_CMD performed better in simulating the temporal variation of AET as a result of changing store levels.

Although this study demonstrates that evapotranspiration process representation within conceptual rainfall-runoff models can substantially affect the results from climate impact assessments, quantitative sensitivity values are likely to vary on a case-by-case basis, depending on the catchment and the choice of PET and rainfall-runoff models. Therefore, specific studies are required for further exploration of the implications of modelling assumptions for a larger number of rainfall-runoff models, as well as their interactions on other case studies. Nevertheless, the results from this study highlight the importance of scrutinizing internal process realism within rainfall-runoff models as part of climate impact studies, and using alternative sources of information on model performance in addition to the standard runoff-based metrics, such as by comparing simulated and observed AET or with the outputs of integrated surface-subsurface flow models [e.g. *Li et al.*, 2015; *Partington et al.*, 2013; *Su et al.*, 2016; *Vervoort et al.*, 2014]).

These findings are in line with a number of studies that suggest the need for an improved understanding of physical processes to better infer the potential changes in rainfall-runoff relationships under climate change, and thus to facilitate better modelling of future water resources [*Fowler et al.*, 2016; *Herman et al.*, 2013; *Kirchner*, 2006; *Merz et al.*, 2011; *Minville et al.*, 2014; *Saft et al.*, 2016; *Westra et al.*, 2014]. The study also provides a practical example of the multiple-hypothesis testing of rainfall-runoff models [*Clark et al.*, *2011; Clark et al., 2016; Gupta et al.*, 2008; *Harrigan et al.*, 2014], which suggests that models should be evaluated based on the validity of any individual hypothesis they describe. With the currently increasing availability of observations to support hypothesis testing [for example see *Blöschl et al.*, 2016], this type of process-based model evaluation can greatly enhance our understanding on how alternative rainfall-runoff models can propagate climate change signals to hydrological impacts via different model conceptualizations and assumptions. As highlighted by the substantially different elasticity values found in this study, these process-based model evaluation studies will be particularly useful to inform the selection of rainfall-runoff models for climate impact studies, where good model performance under historical climate conditions provides only a partial guide as to how the model will perform under changed climate conditions.

ACKNOWLEDGEMENTS

The streamflow data used for the five catchments in this study were from the Australian Bureau of Meteorology's (BOM) Hydrologic Reference Station project website: www.bom.gov.au/hrs [*Bureau of Meteorology*, 2015]. The rainfall, temperature, relative humidity, wind and sunshine hour data for the five weather stations were obtained from the Climate Data Online project website, http://www.bom.gov.au/climate/data/ [*Bureau of Meteorology*, 2016]. The EC-based AET observations for Alice Springs and Wagga Wagga were obtained from the OzFlux website, at http://www.ozflux.org.au/ [*Cleverly*, 2011; *vanGorsel*, 2013]. The authors would also like to thank the three anonymous reviewers, whose comments have helped to improve the quality of this paper significantly.

Tables:

Table 1: Average climate conditions at the five case study locations between 01/01/1995 and 31/12/2003.

Weather station	T_{max} (°C)	T_{min} (°C)	RH_{max} (%)	RH_{min} (%)	*Rs* (MJ/(m^2.day))	u_z (m/s)	Annual PET (mm)	Catchment (and area)	Annual P (mm)	Annual Q (mm)	PET/ P
Adelaide	21.4	12.5	80.2	42.2	16.9	3.16	1372	Scott Creek (29 km^2)	892	133	1.54
Burnie	15.7	12.7	77.1	65.3	14.3	4.05	958	Black River (318.5 km^2)	1182	550	0.81
Darwin	31.2	23.7	88.5	50.1	20.3	3.39	1864	Elizabeth River (95.6 km^2)	1979	777	0.94
Alice Springs	28.5	13.8	65.6	23.5	20.8	2.35	1822	Hugh River (3324 km^2)	344	56.2	5.29
Wagga Wagga	21.6	9.99	83.2	40.3	17.5	3.29	1436	Adelong Creek (146.1 km^2)	799	195	1.80

***Notation: T_{max} = maximum temperature; T_{min} = minimum temperature, R_s = incoming solar radiation, RH_{max} = maximum relative humidity, RH_{min} = minimum relative humidity, u_z = wind speed, PET = potential evapotranspiration calculated using the Penman-Monteith model, P = catchment-average precipitation, Q = average runoff at catchment outlet.**

Table 2: Plausible perturbation ranges for each climate variable relative to their historical levels.

Climate variable to perturb	Perturbation range
T	0 to +8°C
RH	-10% to +10%
R_s	-10% to +10%
u_z	-20% to +20%

Table 3: NSE for calibration and validation for the GR4J, AWBM and IHACRES_CMD models at the five case study sites, with relative bias shown in brackets.

SMA model name	GR4J	AWBM	IHACRES_CMD

Study site	Calibration	Validation	Calibration	Validation	Calibration	Validation
Adelaide	0.861 (0.011)	0.800 (0.025)	0.812 (-0.274)	0.804 (0.292)	0.856 (0.020)	0.809 (-0.028)
Burnie	0.862 (-0.010)	0.869 (-0.053)	0.799 (-0.089)	0.757 (0.018)	0.860 (0.008)	0.868 (-0.070)
Darwin	0.849 (0.052)	0.834 (-0.215)	0.825 (0.013)	0.823 (-0.148)	0.848 (0.048)	0.848 (-0.226)
Alice Springs	0.805 (-0.650)	0.581 (0.034)	0.778 (0.599)	0.569 (-0.737)	0.800 (-0.503)	0.585 (-0.912)
Wagga Wagga	0.748 (-0.072)	0.695 (0.083)	0.513 (-0.096)	0.618 (-0.298)	0.713 (-0.085)	0.642 (0.083)
Average NSE	**0.825**	**0.756**	**0.746**	**0.714**	**0.815**	**0.750**

List of Figures:

Figure 8: Comparison of the observed and simulated time-series of AET from GR4J, AWBM and IHACRES_CMD, at a) Alice Springs; and b) Wagga Wagga.

REFERENCES

Akhtar, M., N. Ahmad, and M. J. Booij (2008), The impact of climate change on the water resources of Hindukush–Karakorum–Himalaya region under different glacier coverage scenarios, *Journal of Hydrology*, *355*(1–4), 148-163.
Allen, R. G., L. S. Pereira, D. Raes, and M. Smith (1998), Crop evapotranspiration-Guidelines for computing crop water requirements-FAO Irrigation and drainage paper 56, *FAO, Rome*, *300*, 6541.
Andréassian, V., C. Perrin, and C. Michel (2004), Impact of imperfect potential evapotranspiration knowledge on the efficiency and parameters of watershed models, *Journal of Hydrology*, *286*(1–4), 19-35.
Andrews, F., and J. Guillaume (2013), hydromad: Hydrological Model Assessment and Development. R package version 0.9-18., edited.
Arnell, N. W. (2004), Climate-change impacts on river flows in Britain: the UKCIPO2 scenarios, *Water and Environment Journal*, *18*(2), 112-117.
Bae, D.-H., I.-W. Jung, and D. P. Lettenmaier (2011), Hydrologic uncertainties in climate change from IPCC AR4 GCM simulations of the Chungju Basin, Korea, *Journal of Hydrology*, *401*(1–2), 90-105.
Bastola, S., C. Murphy, and J. Sweeney (2011), The role of hydrological modelling uncertainties in climate change impact assessments of Irish river catchments, *Advances in Water Resources*, *34*(5), 562-576.
Bethune, M., N. Austin, and S. Maher (2001), Quantifying the water budget of irrigated rice in the Shepparton Irrigation Region, Australia, *Irrigation Science*, *20*(3), 99-105.
Beven, K. J. (2001a), On hypothesis testing in hydrology, *Hydrological processes*, *15*(9), 1655-1657.
Beven, K. J. (2001b), How far can we go in distributed hydrological modelling?, *Hydrology and Earth System Sciences Discussions*, *5*(1), 1-12.
Beven, K. J. (2011), *Rainfall-Runoff Modelling: The Primer*, Wiley.
Blöschl, G., et al. (2016), The Hydrological Open Air Laboratory (HOAL) in Petzenkirchen: a hypothesis-driven observatory, *Hydrol. Earth Syst. Sci.*, *20*(1), 227-255.
Boughton, W. (2004), The Australian water balance model, *Environmental Modelling & Software*, *19*(10), 943-956.
Boughton, W. (2009), New approach to calibration of the AWBM for use on ungauged catchments, *Journal Of Hydrologic Engineering*, *14*(6), 562-568.
Brouyère, S., G. Carabin, and A. Dassargues (2004), Climate change impacts on groundwater resources: modelled deficits in a chalky aquifer, Geer basin, Belgium, *Hydrogeology Journal*, *12*(2), 123-134.
Bureau of Meteorology (2015), Hydrologic Reference Stations, edited.
Bureau of Meteorology (2016), Climate Data Online, edited.
Butts, M. B., J. T. Payne, M. Kristensen, and H. Madsen (2004), An evaluation of the impact of model structure on hydrological modelling uncertainty for streamflow simulation, *Journal of Hydrology*, *298*(1–4), 242-266.
Chapman, T. G. "Estimation of evaporation in rainfall-runoff models."*Proceedings MODSIM 2003 International Congress on Modelling and Simulation*. Vol. 1. Modelling and Simulation Society of Australia, 2003.
Chiew, F. H. S. (2006), Estimation of rainfall elasticity of streamflow in Australia, *Hydrological Sciences Journal*, *51*(4), 613-625.

Chiew, F. H. S., and T. A. McMahon (1991), The applicability of Morton's and Penman's evapotranspiration estimates in rainfall-runoff modelling, *JAWRA Journal of the American Water Resources Association*, *27*(4), 611-620.
Chiew, F. H. S., J. Teng, J. Vaze, D. A. Post, J. M. Perraud, D. G. C. Kirono, and N. R. Viney (2009), Estimating climate change impact on runoff across southeast Australia: Method, results, and implications of the modeling method, *Water Resources Research*, *45*(10), W10414.
Chiew, F. H. S., D. G. C. Kirono, D. M. Kent, A. J. Frost, S. P. Charles, B. Timbal, K. C. Nguyen, and G. Fu (2010), Comparison of runoff modelled using rainfall from different downscaling methods for historical and future climates, *Journal of Hydrology*, *387*(1–2), 10-23.
Christensen, N. S., A. W. Wood, N. Voisin, D. P. Lettenmaier, and R. N. Palmer (2004), The Effects of Climate Change on the Hydrology and Water Resources of the Colorado River Basin, *Climatic Change*, *62*(1), 337-363.
Clark, M. P., D. Kavetski, and F. Fenicia (2011), Pursuing the method of multiple working hypotheses for hydrological modeling, *Water Resources Research*, *47*(9), W09301.
Clark, M.P., Wilby, R.L., Gutmann, E.D., Vano, J.A., Gangopadhyay, S., Wood, A.W., Fowler, H.J., Prudhomme, C., Arnold, J.R.Brekke, L.D. (2016), 'Characterizing Uncertainty of the Hydrologic Impacts of Climate Change', *Current Climate Change Reports*, vol. 2, no. 2, pp. 55-64.
Cleugh, H. A., R. Leuning, Q. Mu, and S. W. Running (2007), Regional evaporation estimates from flux tower and MODIS satellite data, *Remote Sensing of Environment*, *106*(3), 285-304.
Cleverly, J. (2011), Alice Springs Mulga OzFlux site OzFlux, edited.
Coron, L., V. Andréassian, C. Perrin, J. Lerat, J. Vaze, M. Bourqui, and F. Hendrickx (2012), Crash testing hydrological models in contrasted climate conditions: An experiment on 216 Australian catchments, *Water Resources Research*, *48*(5), n/a-n/a.
Croke, B. F. W., and A. J. Jakeman (2004), A catchment moisture deficit module for the IHACRES rainfall-runoff model, *Environmental Modelling and Software with Environment Data News*, *19*(1), 1-5.
Crossman, J., M. N. Futter, S. K. Oni, P. G. Whitehead, L. Jin, D. Butterfield, H. M. Baulch, and P. J. Dillon (2013), Impacts of climate change on hydrology and water quality: Future proofing management strategies in the Lake Simcoe watershed, Canada, *Journal of Great Lakes Research*, *39*(1), 19-32.
CSIRO and Bureau of Meteorology (2015), Climate Change in Australia Information for Australia's Natural Resource Management Regions: Technical Report, CSIRO and Bureau of Meteorology, Australia.
Dingman, S. L. (2015), *Physical Hydrology: Third Edition*, Waveland Press.
Ewen, J., G. O'Donnell, A. Burton, and E. O'Connell (2006), Errors and uncertainty in physically-based rainfall-runoff modelling of catchment change effects, *Journal of Hydrology*, *330*(3–4), 641-650.
Fowler, K. J. A., M. C. Peel, A. W. Western, L. Zhang, and T. J. Peterson (2016), Simulating runoff under changing climatic conditions: Revisiting an apparent deficiency of conceptual rainfall-runoff models, *Water Resources Research*, *52*(3), 1820-1846.
Goderniaux, P., S. Brouyère, H. J. Fowler, S. Blenkinsop, R. Therrien, P. Orban, and A. Dassargues (2009), Large scale surface–subsurface hydrological model to assess climate change impacts on groundwater reserves, *Journal of Hydrology*, *373*(1–2), 122-138.

Gong, L., C.-y. Xu, D. Chen, S. Halldin, and Y. D. Chen (2006), Sensitivity of the Penman–Monteith reference evapotranspiration to key climatic variables in the Changjiang (Yangtze River) basin, *Journal of Hydrology*, *329*(3–4), 620-629.
Gosling, S. N., R. G. Taylor, N. W. Arnell, and M. C. Todd (2011), A comparative analysis of projected impacts of climate change on river runoff from global and catchment-scale hydrological models, *Hydrol. Earth Syst. Sci.*, *15*(1), 279-294.
Goyal, R. K. (2004), Sensitivity of evapotranspiration to global warming: a case study of arid zone of Rajasthan (India), *Agricultural Water Management*, *69*(1), 1-11.
Guo, D., S. Westra, and H. R. Maier (2016), An R package for modelling actual, potential and reference evapotranspiration, *Environmental Modelling & Software*, *78*, 216-224.
Guo, D., S. Westra, and H. R. Maier (2016), Sensitivity of potential evapotranspiration to changes in climate variables for different climatic zones, *Hydrol. Earth Syst. Sci. Discuss.*, doi:10.5194/hess-2016-441, in review.
Gupta, H. V., T. Wagener, and Y. Liu (2008), Reconciling theory with observations: elements of a diagnostic approach to model evaluation, *Hydrological Processes*, *22*(18), 3802-3813.
Haque, M. M., A. Rahman, D. Hagare, G. Kibria, and F. Karim (2015), Estimation of catchment yield and associated uncertainties due to climate change in a mountainous catchment in Australia, *Hydrological Processes*, *29*(19), 4339-4349.
Harrigan, S., C. Murphy, J. Hall, R. L. Wilby, and J. Sweeney (2014), Attribution of detected changes in streamflow using multiple working hypotheses, *Hydrol. Earth Syst. Sci.*, *18*(5), 1935-1952.
Hartmann, G., and A. Bárdossy (2005), Investigation of the transferability of hydrological models and a method to improve model calibration, *Advances in Geosciences*, *5*, 83-87.
Hauser, R., S. Archer, P. Backlund, J. Hatfield, A. Janetos, D. Lettenmaier, and M. Walsh (2009), The effects of climate change on US Ecosystems, *US Global Change Research Program*.
Herman, J. D., P. M. Reed, and T. Wagener (2013), Time-varying sensitivity analysis clarifies the effects of watershed model formulation on model behavior, *Water Resources Research*, *49*(3), 1400-1414.
Huo, Z., X. Dai, S. Feng, S. Kang, and G. Huang (2013), Effect of climate change on reference evapotranspiration and aridity index in arid region of China, *Journal of Hydrology*, *492*, 24-34.
Ibrom, A., E. Dellwik, H. Flyvbjerg, N. O. Jensen, and K. Pilegaard (2007), Strong low-pass filtering effects on water vapour flux measurements with closed-path eddy correlation systems, *Agricultural and Forest Meteorology*, *147*(3–4), 140-156.
IPCC (2014), Climate Change 2014: Impacts, Adaptation, and Vulnerability. Part A: Global and Sectoral Aspects. Contribution of Working Group II to the Fifth Assessment Report of the Intergovernmental Panel on Climate Change, 1132 pp, Cambridge, United Kingdom and New York, NY, USA.
Islam, S. A., M. A. Bari, and A. H. M. F. Anwar (2014), Hydrologic impact of climate change on Murray–Hotham catchment of Western Australia: a projection of rainfall–runoff for future water resources planning, *Hydrol. Earth Syst. Sci.*, *18*(9), 3591-3614.
Jiang, T., Y. D. Chen, C.-y. Xu, X. Chen, X. Chen, and V. P. Singh (2007), Comparison of hydrological impacts of climate change simulated by six hydrological models in the Dongjiang Basin, South China, *Journal of Hydrology*, *336*(3–4), 316-333.
Kay, A. L., and R. G. Jones (2012), Comparison of the use of alternative UKCP09 products for modelling the impacts of climate change on flood frequency, *Climatic Change*, *114*(2), 211-230.

Kay, A. L., H. N. Davies, V. A. Bell, and R. G. Jones (2009), Comparison of uncertainty sources for climate change impacts: flood frequency in England, *Climatic Change*, *92*(1-2), 41-63.
Kirchner, J. W. (2006), Getting the right answers for the right reasons: Linking measurements, analyses, and models to advance the science of hydrology, *Water Resources Research*, *42*(3), n/a-n/a.
Klemeš, V. (1986), Operational testing of hydrological simulation models, *Hydrological Sciences Journal*, *31*(1), 13-24.
Li, L., M. F. Lambert, H. R. Maier, D. Partington, and C. T. Simmons (2015), Assessment of the internal dynamics of the Australian Water Balance Model under different calibration regimes, *Environmental Modelling & Software*, *66*, 57-68.
Mendoza, P.A., Clark, M.P., Mizukami, N., Gutmann, E.D., Arnold, J.R., Brekke, L.D.Rajagopalan, B. (2016), How do hydrologic modeling decisions affect the portrayal of climate change impacts?, *Hydrological Processes,* vol. 30, no. 7, pp. 1071-1095.
McKenney, M. S., and N. J. Rosenberg (1993), Sensitivity of some potential evapotranspiration estimation methods to climate change, *Agricultural and Forest Meteorology*, *64*(1–2), 81-110.
McMahon, T. A., M. C. Peel, L. Lowe, R. Srikanthan, and T. R. McVicar (2013), Estimating actual, potential, reference crop and pan evaporation using standard meteorological data: a pragmatic synthesis, *Hydrol. Earth Syst. Sci.*, *17*(4), 1331-1363.
Meiresonne, L., D. A. Sampson, A. S. Kowalski, I. A. Janssens, N. Nadezhdina, J. Cermák, J. Van Slycken, and R. Ceulemans (2003), Water flux estimates from a Belgian Scots pine stand: a comparison of different approaches, *Journal of Hydrology*, *270*(3–4), 230-252.
Merz, R., J. Parajka, and G. Blöschl (2011), Time stability of catchment model parameters: Implications for climate impact analyses, *Water Resources Research*, *47*(2), n/a-n/a.
Meyer, W. S., E. Kondrlovà, and G. R. Koerber (2015), Evaporation of perennial semi-arid woodland in southeastern Australia is adapted for irregular but common dry periods, *Hydrological Processes*, *29*(17), 3714-3726.
Minville, M., D. Cartier, C. Guay, L.-A. Leclaire, C. Audet, S. Le Digabel, and J. Merleau (2014), Improving process representation in conceptual hydrological model calibration using climate simulations, *Water Resources Research*, *50*(6), 5044-5073.
Mu, Q., M. Zhao, and S. W. Running (2011), Improvements to a MODIS global terrestrial evapotranspiration algorithm, *Remote Sensing of Environment*, *115*(8), 1781-1800.
Najafi, M. R., and H. Moradkhani (2015), Multi-model ensemble analysis of runoff extremes for climate change impact assessments, *Journal of Hydrology*, *525*, 352-361.
Northey, J. E., E. W. Christen, J. E. Ayars, and J. Jankowski (2006), Occurrence and measurement of salinity stratification in shallow groundwater in the Murrumbidgee Irrigation Area, south-eastern Australia, *Agricultural Water Management*, *81*(1–2), 23-40.
New, M., Lopez, A., Dessai, S.Wilby, R. (2007), Challenges in using probabilistic climate change information for impact assessments: an example from the water sector, *Philosophical Transactions of the Royal Society A: Mathematical, Physical and Engineering Sciences*, vol. 365, no. 1857, pp. 2117-2131.
Oudin, L., C. Michel, and F. Anctil (2005), Which potential evapotranspiration input for a lumped rainfall-runoff model?: Part 1—Can rainfall-runoff models effectively handle detailed potential evapotranspiration inputs?, *Journal of Hydrology*, *303*(1–4), 275-289.
Oudin, L., C. Perrin, T. Mathevet, V. Andréassian, and C. Michel (2006), Impact of biased and randomly corrupted inputs on the efficiency and the parameters of watershed models, *Journal of Hydrology*, *320*(1–2), 62-83.

Partington, D., P. Brunner, S. Frei, C. T. Simmons, A. D. Werner, R. Therrien, H. R. Maier, G. C. Dandy, and J. H. Fleckenstein (2013), Interpreting streamflow generation mechanisms from integrated surface-subsurface flow models of a riparian wetland and catchment, *Water Resources Research*, *49*(9), 5501-5519.
Paton, F. L., H. R. Maier, and G. C. Dandy (2013), Relative magnitudes of sources of uncertainty in assessing climate change impacts on water supply security for the southern Adelaide water supply system, *Water Resources Research*, *49*(3), 1643-1667.
Paton, F. L., H. R. Maier, and G. C. Dandy (2014), Including adaptation and mitigation responses to climate change in a multiobjective evolutionary algorithm framework for urban water supply systems incorporating GHG emissions, *Water Resources Research*, *50*(8), 6285-6304.
Perrin, C., C. Michel, and V. Andréassian (2003), Improvement of a parsimonious model for streamflow simulation, *Journal of hydrology*, *279*(1), 275-289.
Perrin, C., V. Andréassian, C. Michel, and L. Oudin (2005), GR4J: a parsimonious model for rainfall-runoff simulations, paper presented at Geophysical Research Abstracts.
Saft, M., M. C. Peel, A. W. Western, J.-M. Perraud, and L. Zhang (2016), Bias in streamflow projections due to climate-induced shifts in catchment response, *Geophysical Research Letters*, *43*(4), 1574-1581.
Seibert, J., and J. J. McDonnell (2002), On the dialog between experimentalist and modeler in catchment hydrology: Use of soft data for multicriteria model calibration, *Water Resources Research*, *38*(11), 23-21-23-14.
Seibert, J., A. Rodhe, and K. Bishop (2003), Simulating interactions between saturated and unsaturated storage in a conceptual runoff model, *Hydrological Processes*, *17*(2), 379-390.
Seneviratne, S. I., et al. (2012), Swiss prealpine Rietholzbach research catchment and lysimeter: 32 year time series and 2003 drought event, *Water Resources Research*, *48*(6), n/a-n/a.
Stern, H., G. De Hoedt, and J. Ernst (2000), Objective classification of Australian climates, *Australian Meteorological Magazine*, *49*(2), 87-96.
Stocker, T. F., D. Qin, G.-K. Plattner, M. Tignor, S. K. Allen, J. Boschung, A. Nauels, Y. Xia, V. Bex, and P. M. Midgley (2013), Climate change 2013: The physical science basis, *Intergovernmental Panel on Climate Change, Working Group I Contribution to the IPCC Fifth Assessment Report (AR5)(Cambridge Univ Press, New York)*.
Su, C.-H., J. F. Costelloe, T. J. Peterson, and A. W. Western (2016), On the structural limitations of recursive digital filters for base flow estimation, *Water Resources Research*, *52*(6), 4745-4764.
TERN (2012), Coping with complex data streams: the OzFlux approach, *TERN e-Newsletter*.
Turral, H., J. Burke, and J.-M. Faurès (2011), *Climate change, water and food security*, FAO.
Teng, J., Vaze, J., Chiew, F.H.S., Wang, B.Perraud, J.-M. (2012), Estimating the Relative Uncertainties Sourced from GCMs and Hydrological Models in Modeling Climate Change Impact on Runoff, *Journal of Hydrometeorology*, vol. 13, no. 1, pp. 122-139.
vanGorsel, E. (2013), Tumbarumba OzFlux tower site OzFlux, edited.
Vaze, J., and J. Teng (2011), Future climate and runoff projections across New South Wales, Australia: results and practical applications, *Hydrological Processes*, *25*(1), 18-35.
Vaze, J., D. A. Post, F. H. S. Chiew, J. M. Perraud, N. R. Viney, and J. Teng (2010), Climate non-stationarity – Validity of calibrated rainfall–runoff models for use in climate change studies, *Journal of Hydrology*, *394*(3–4), 447-457.
Velázquez, J. A., J. Schmid, S. Ricard, M. J. Muerth, B. Gauvin St-Denis, M. Minville, D. Chaumont, D. Caya, R. Ludwig, and R. Turcotte (2013), An ensemble approach to assess

hydrological models' contribution to uncertainties in the analysis of climate change impact on water resources, *Hydrol. Earth Syst. Sci.*, *17*(2), 565-578.
Vervoort, W. R., S. F. Miechels, F. F. van Ogtrop, and J. H. A. Guillaume (2014), Remotely sensed evapotranspiration to calibrate a lumped conceptual model: Pitfalls and opportunities, *Journal of Hydrology*, *519, Part D*, 3223-3236.
Vicente-Serrano, S. M., C. Azorin-Molina, A. Sanchez-Lorenzo, J. Revuelto, E. Morán-Tejeda, J. I. López-Moreno, and F. Espejo (2014), Sensitivity of reference evapotranspiration to changes in meteorological parameters in Spain (1961–2011), *Water Resources Research*, *50*(11), 8458-8480.
Wagener, T., N. McIntyre, M. J. Lees, H. S. Wheater, and H. V. Gupta (2003), Towards reduced uncertainty in conceptual rainfall-runoff modelling: dynamic identifiability analysis, *Hydrological Processes*, *17*(2), 455-476.
Wang, K., and R. E. Dickinson (2012), A review of global terrestrial evapotranspiration: Observation, modeling, climatology, and climatic variability, *Reviews of Geophysics*, *50*(2).
Westra, S., M. Thyer, M. Leonard, D. Kavetski, and M. Lambert (2014), A strategy for diagnosing and interpreting hydrological model nonstationarity, *Water Resources Research*, *50*(6), 5090-5113.
Wilson, K. B., P. J. Hanson, P. J. Mulholland, D. D. Baldocchi, and S. D. Wullschleger (2001), A comparison of methods for determining forest evapotranspiration and its components: sap-flow, soil water budget, eddy covariance and catchment water balance, *Agricultural and Forest Meteorology*, *106*(2), 153-168.
Zhang, L., W. R. Dawes, P. G. Slavich, W. S. Meyer, P. J. Thorburn, D. J. Smith, and G. R. Walker (1999), Growth and ground water uptake responses of lucerne to changes in groundwater levels and salinity: lysimeter, isotope and modelling studies, *Agricultural Water Management*, *39*(2–3), 265-282.

Figure 1.

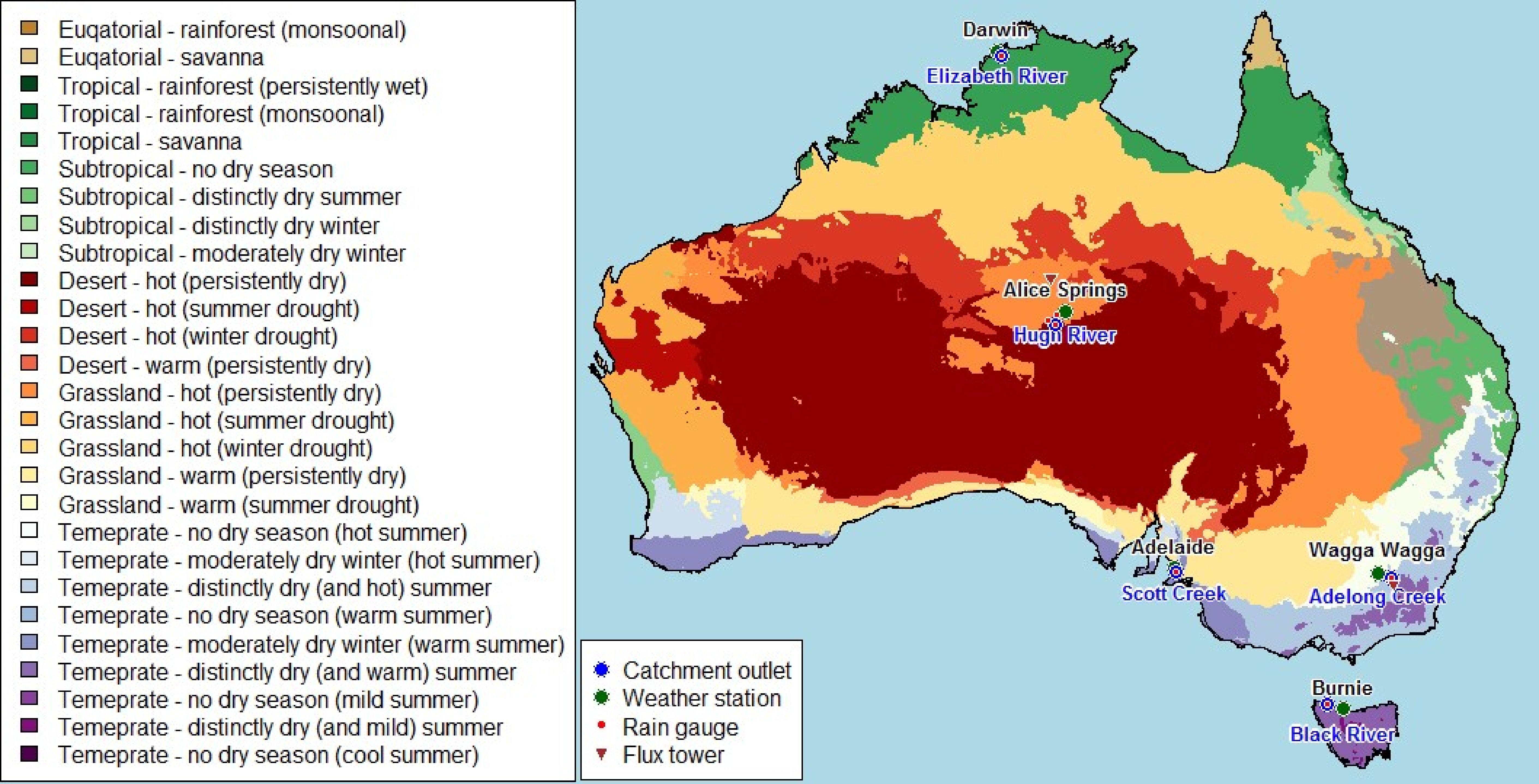

Euqatorial - rainforest (monsoonal)
Euqatorial - savanna
Tropical - rainforest (persistently wet)
Tropical - rainforest (monsoonal)
Tropical - savanna
Subtropical - no dry season
Subtropical - distinctly dry summer
Subtropical - distinctly dry winter
Subtropical - moderately dry winter
Desert - hot (persistently dry)
Desert - hot (summer drought)
Desert - hot (winter drought)
Desert - warm (persistently dry)
Grassland - hot (persistently dry)
Grassland - hot (summer drought)
Grassland - hot (winter drought)
Grassland - warm (persistently dry)
Grassland - warm (summer drought)
Temeprate - no dry season (hot summer)
Temeprate - moderately dry winter (hot summer)
Temeprate - distinctly dry (and hot) summer
Temeprate - no dry season (warm summer)
Temeprate - moderately dry winter (warm summer)
Temeprate - distinctly dry (and warm) summer
Temeprate - no dry season (mild summer)
Temeprate - distinctly dry (and mild) summer
Temeprate - no dry season (cool summer)
Catchment outlet
Weather station
Rain gauge
Flux tower
Darwin
Elizabeth River
Alice Springs
Hugh River
Adelaide
Scott Creek
Wagga Wagga
Adelong Creek
Burnie
Black River

Figure 2.

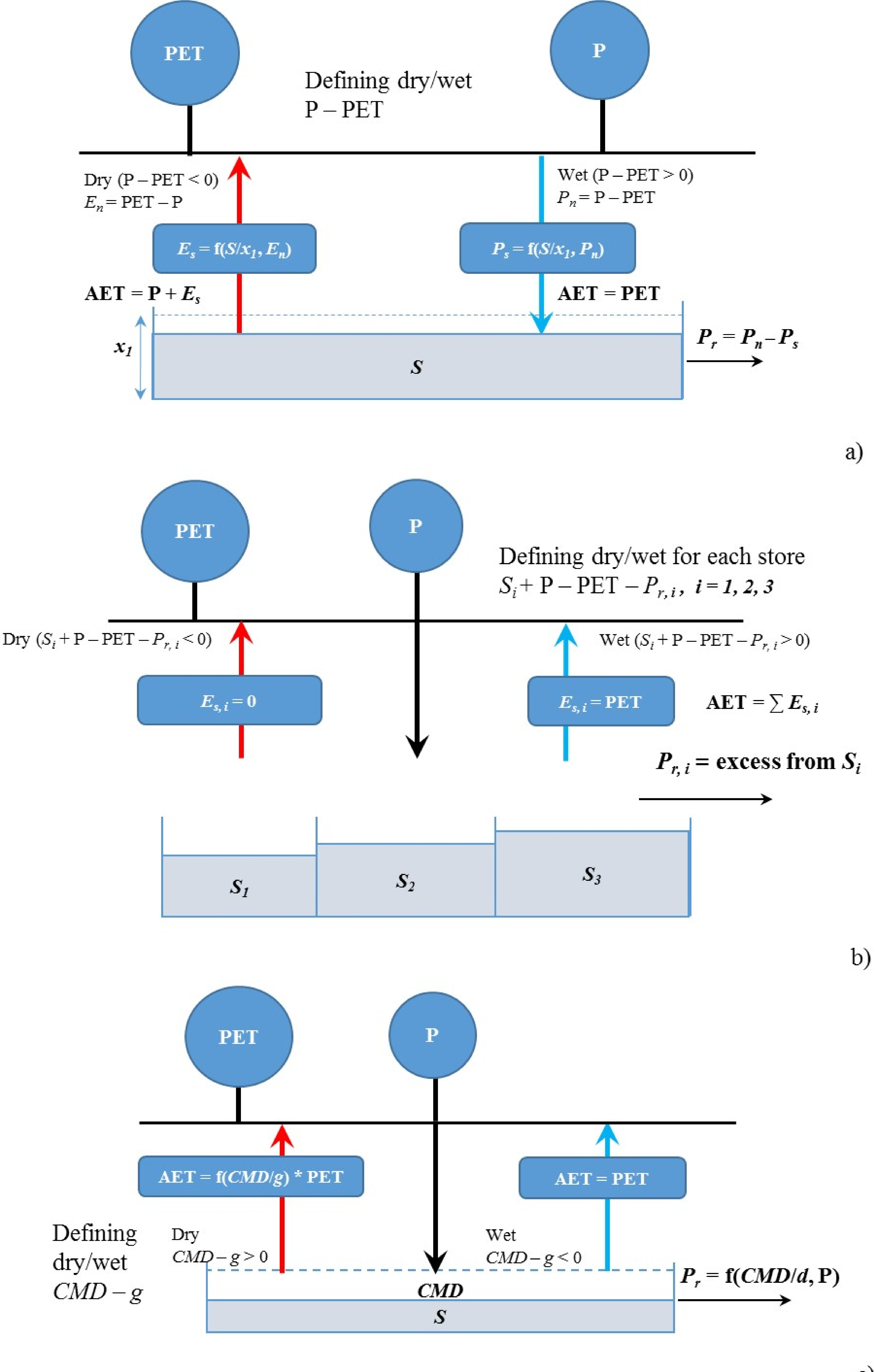
PET
P
Defining dry/wet
P – PET
Dry (P – PET < 0)
E_n = PET – P
Wet (P – PET > 0)
P_n = P – PET
E_s = f(S/x_1, E_n)
P_s = f(S/x_1, P_n)
AET = P + E_s
AET = PET
x_1
S
$P_r = P_n - P_s$
a)
PET
P
Defining dry/wet for each store
S_i + P – PET – $P_{r,i}$, $i = 1, 2, 3$
Dry (S_i + P – PET – $P_{r,i}$ < 0)
Wet (S_i + P – PET – $P_{r,i}$ > 0)
$E_{s,i}$ = 0
$E_{s,i}$ = PET
AET = $\sum E_{s,i}$
$P_{r,i}$ = excess from S_i
S_1
S_2
S_3
b)
PET
P
AET = f(CMD/g) * PET
AET = PET
Defining dry/wet
$CMD - g$
Dry
$CMD - g > 0$
Wet
$CMD - g < 0$
CMD
S
P_r = f(CMD/d, P)
c)

Figure 3.

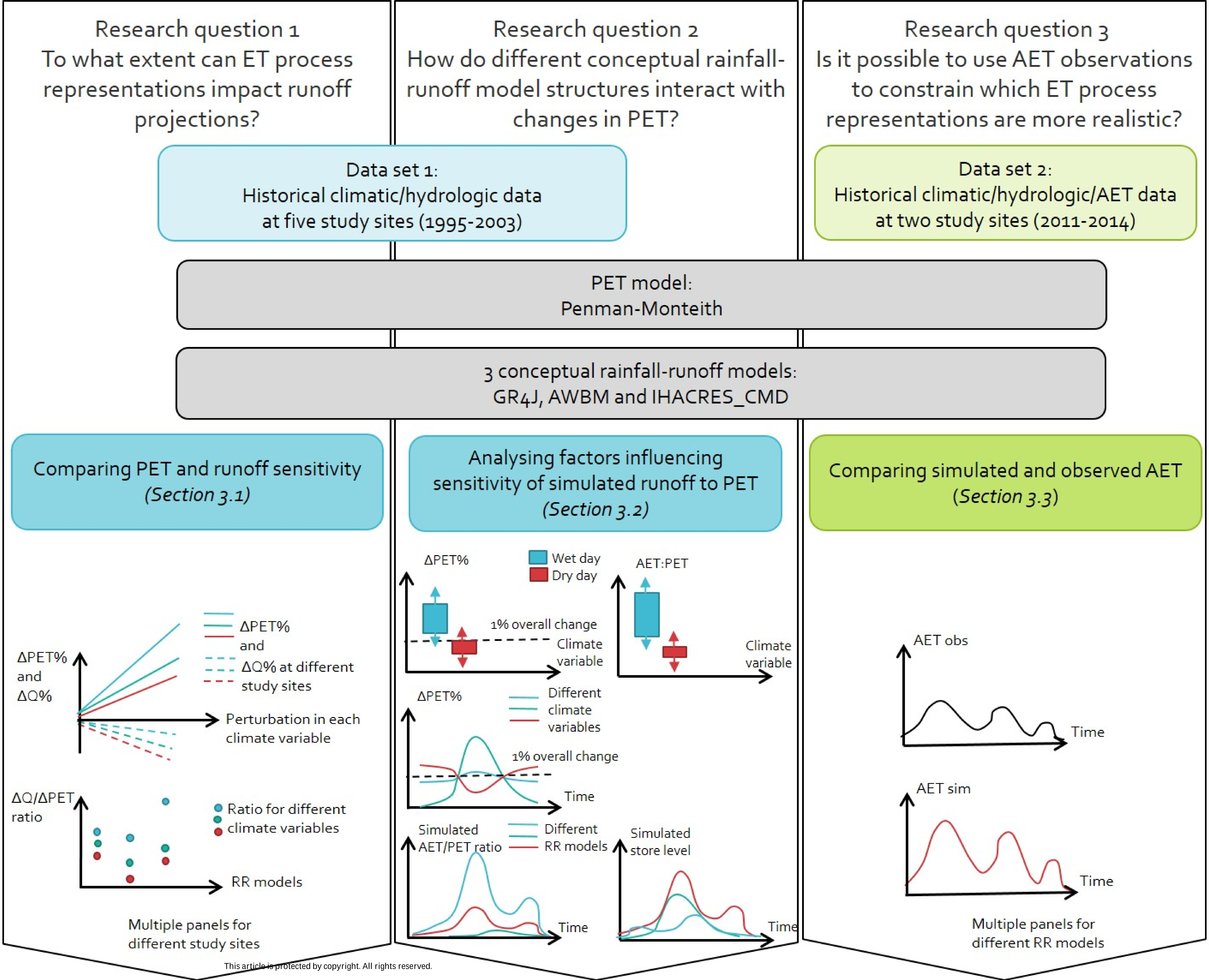

Research question 1
To what extent can ET process representations impact runoff projections?
Research question 2
How do different conceptual rainfall-runoff model structures interact with changes in PET?
Research question 3
Is it possible to use AET observations to constrain which ET process representations are more realistic?
Data set 1:
Historical climatic/hydrologic data at five study sites (1995-2003)
Data set 2:
Historical climatic/hydrologic/AET data at two study sites (2011-2014)
PET model:
Penman-Monteith
3 conceptual rainfall-runoff models:
GR4J, AWBM and IHACRES_CMD
Comparing PET and runoff sensitivity (Section 3.1)
Analysing factors influencing sensitivity of simulated runoff to PET (Section 3.2)
Comparing simulated and observed AET (Section 3.3)
ΔPET% and ΔQ%
ΔPET% and ΔQ% at different study sites
Perturbation in each climate variable
ΔQ/ΔPET ratio
Ratio for different climate variables
RR models
Multiple panels for different study sites
ΔPET%
Wet day
Dry day
1% overall change
Climate variable
AET:PET
Climate variable
ΔPET%
Different climate variables
1% overall change
Time
Simulated AET/PET ratio
Different RR models
Time
Simulated store level
Time
AET obs
Time
AET sim
Time
Multiple panels for different RR models

Figure 4.

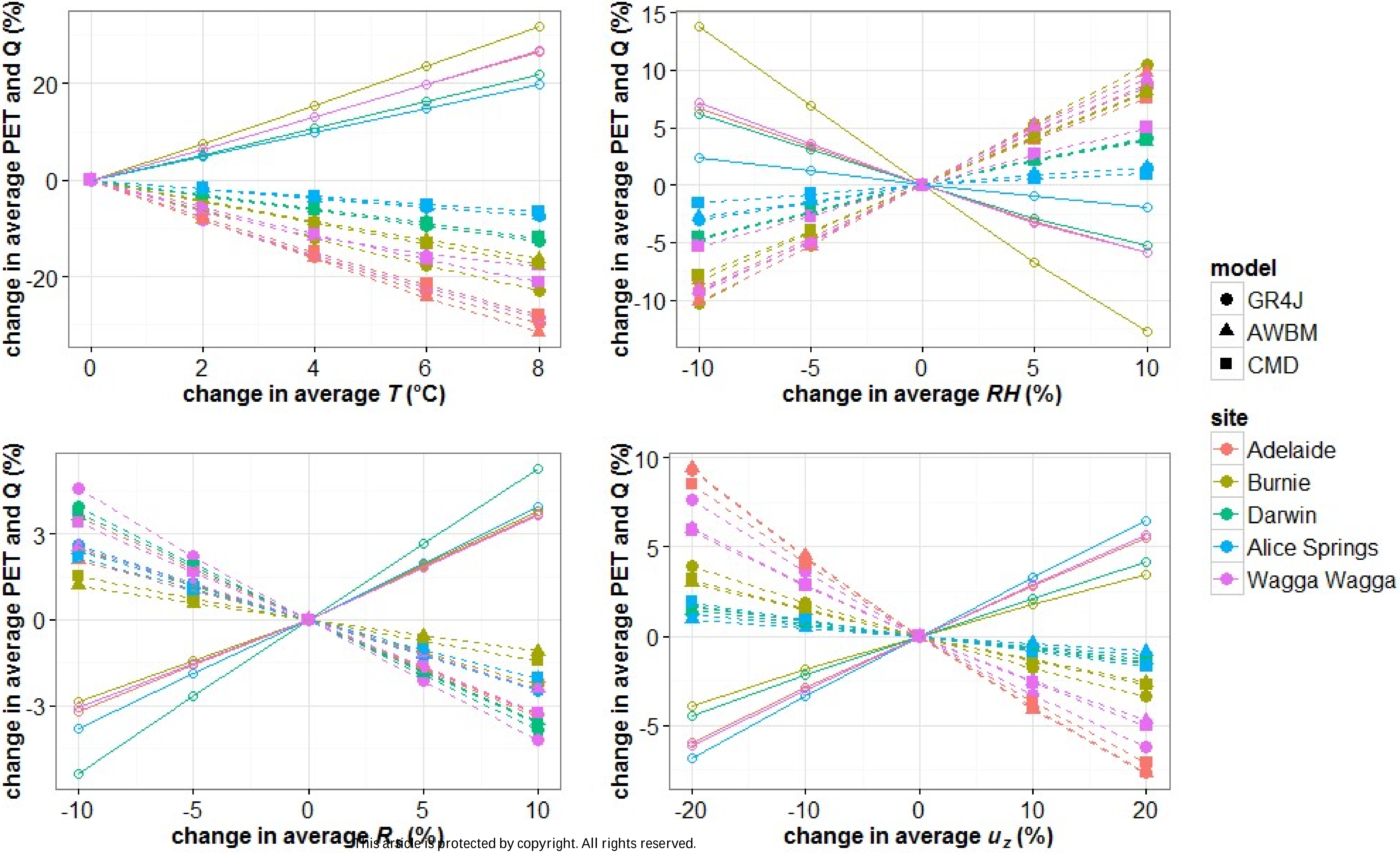
change in average PET and Q (%)
change in average T (°C)
change in average RH (%)
change in average R (%)
change in average u_z (%)
model
GR4J
AWBM
CMD
site
Adelaide
Burnie
Darwin
Alice Springs
Wagga Wagga

Figure 5.

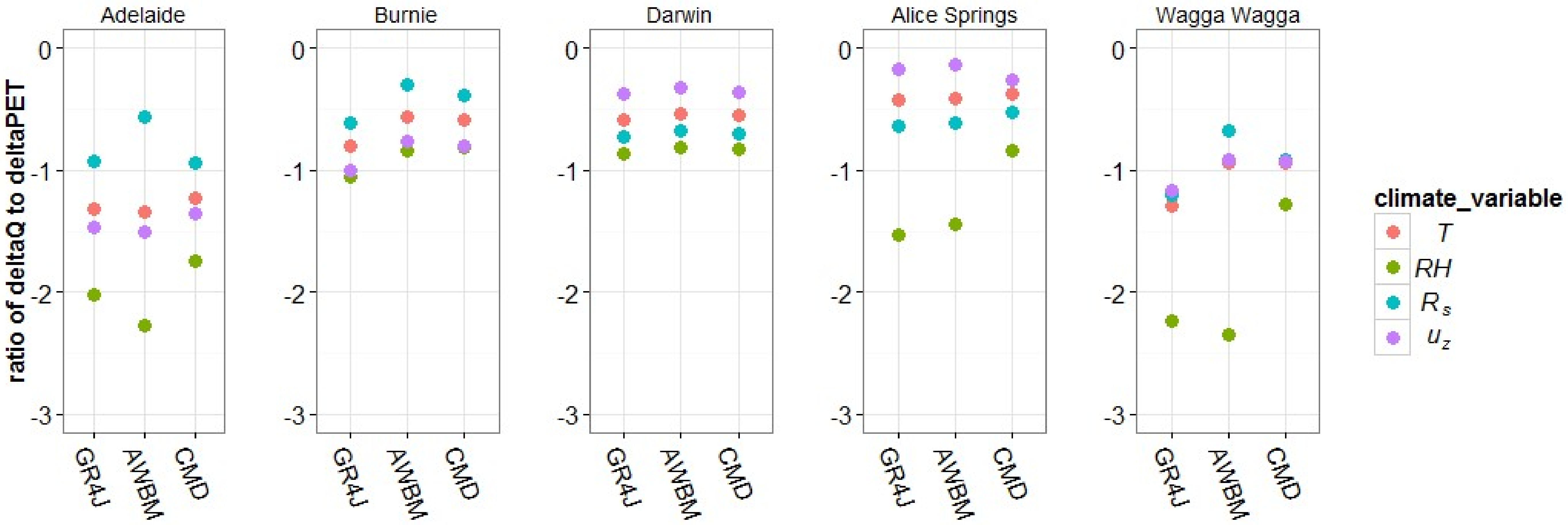
Adelaide
Burnie
Darwin
Alice Springs
Wagga Wagga
ratio of deltaQ to deltaPET
0
-1
-2
-3
GR4J
AWBM
CMD
climate_variable
T
RH
R_s
u_z

Figure 6.

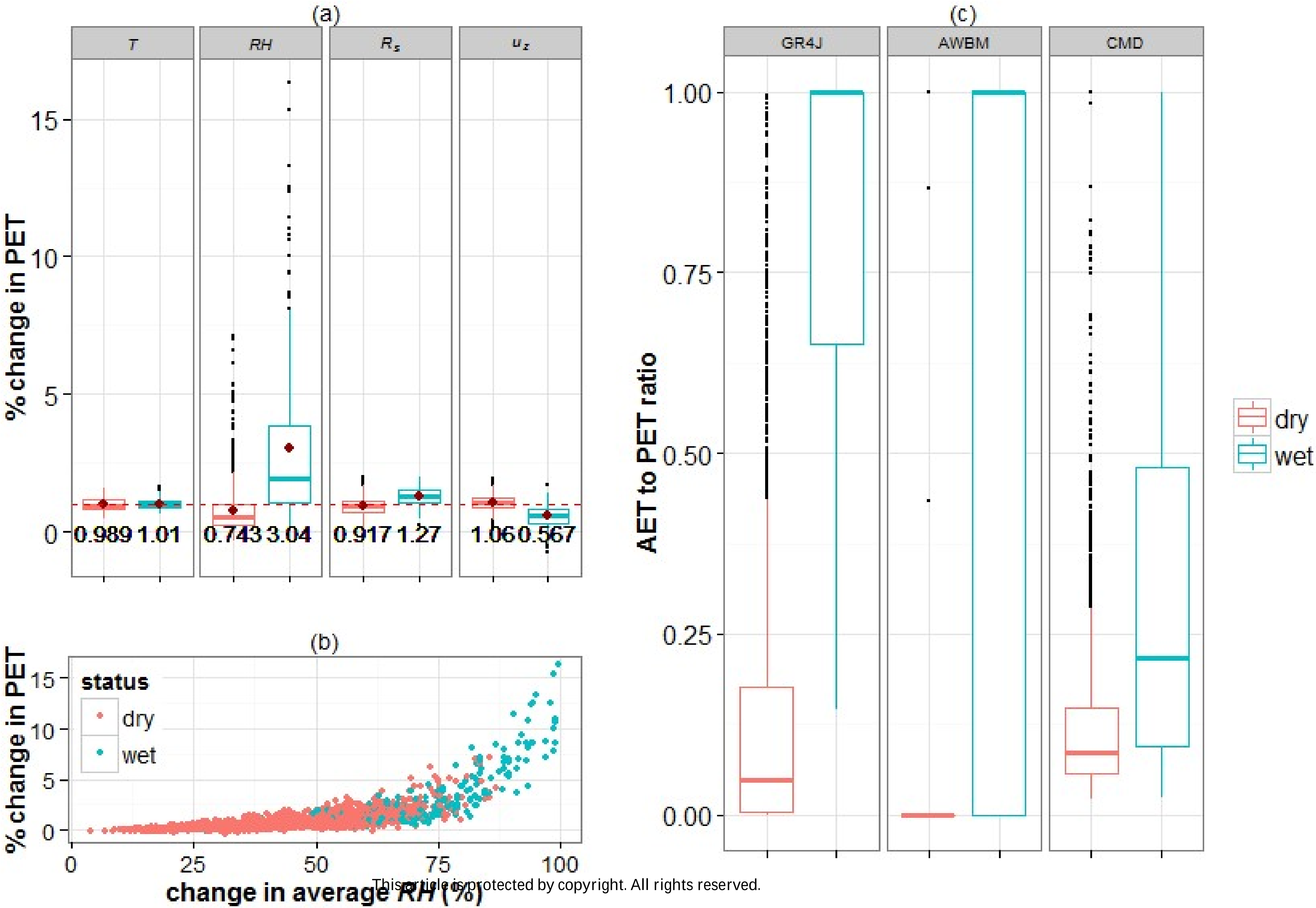
(a)
T
RH
R_s
u_z
% change in PET
0.989 1.01
0.743 3.04
0.917 1.27
1.06 0.567
(b)
status
dry
wet
change in average RH (%)
(c)
GR4J
AWBM
CMD
AET to PET ratio
dry
wet

Figure 7.

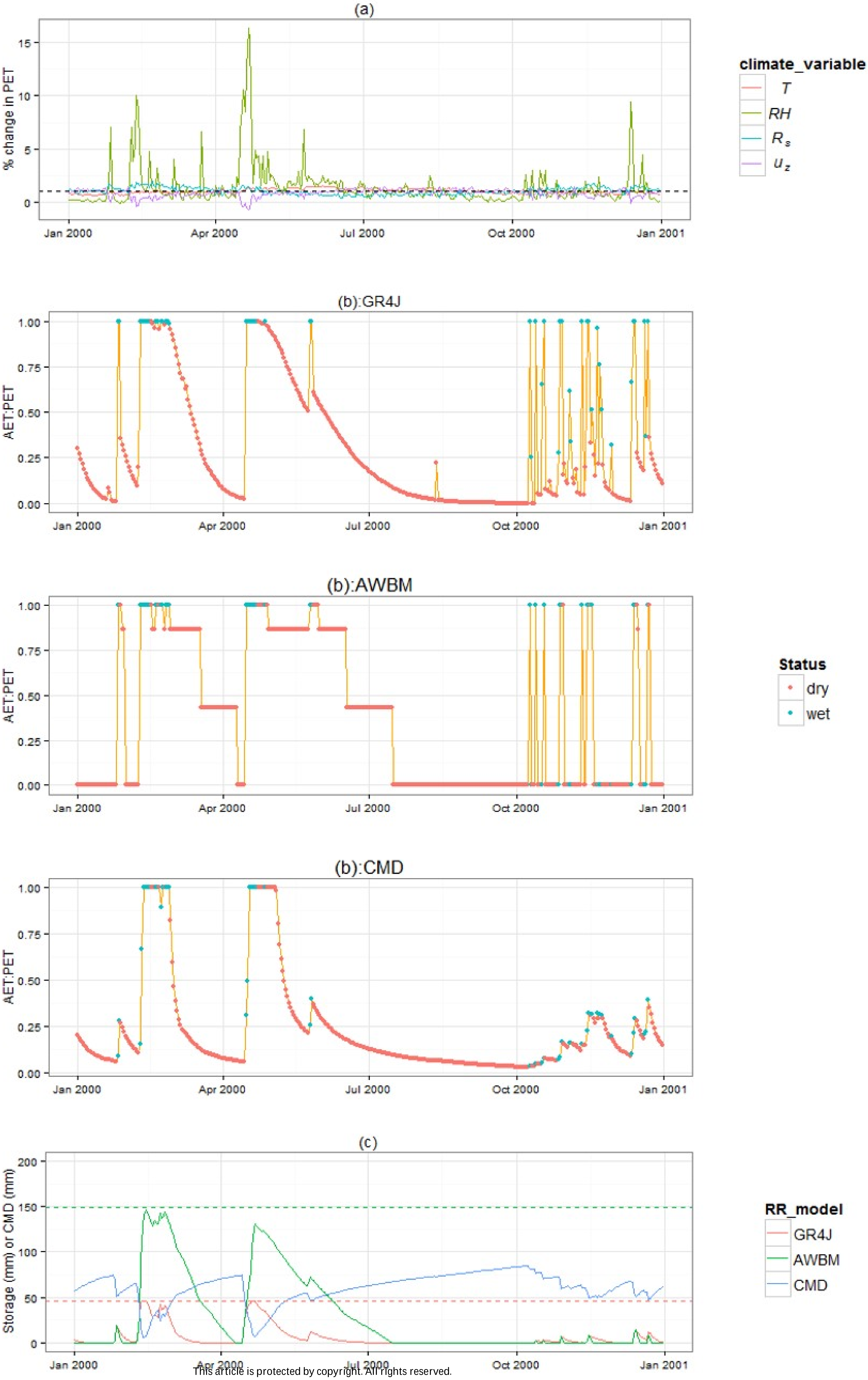

(a)
% change in PET
climate_variable
T
RH
R_s
u_z
(b):GR4J
AET:PET
(b):AWBM
(b):CMD
Status
dry
wet
(c)
Storage (mm) or CMD (mm)
RR_model
GR4J
AWBM
CMD
Jan 2000
Apr 2000
Jul 2000
Oct 2000
Jan 2001

Figure 8.

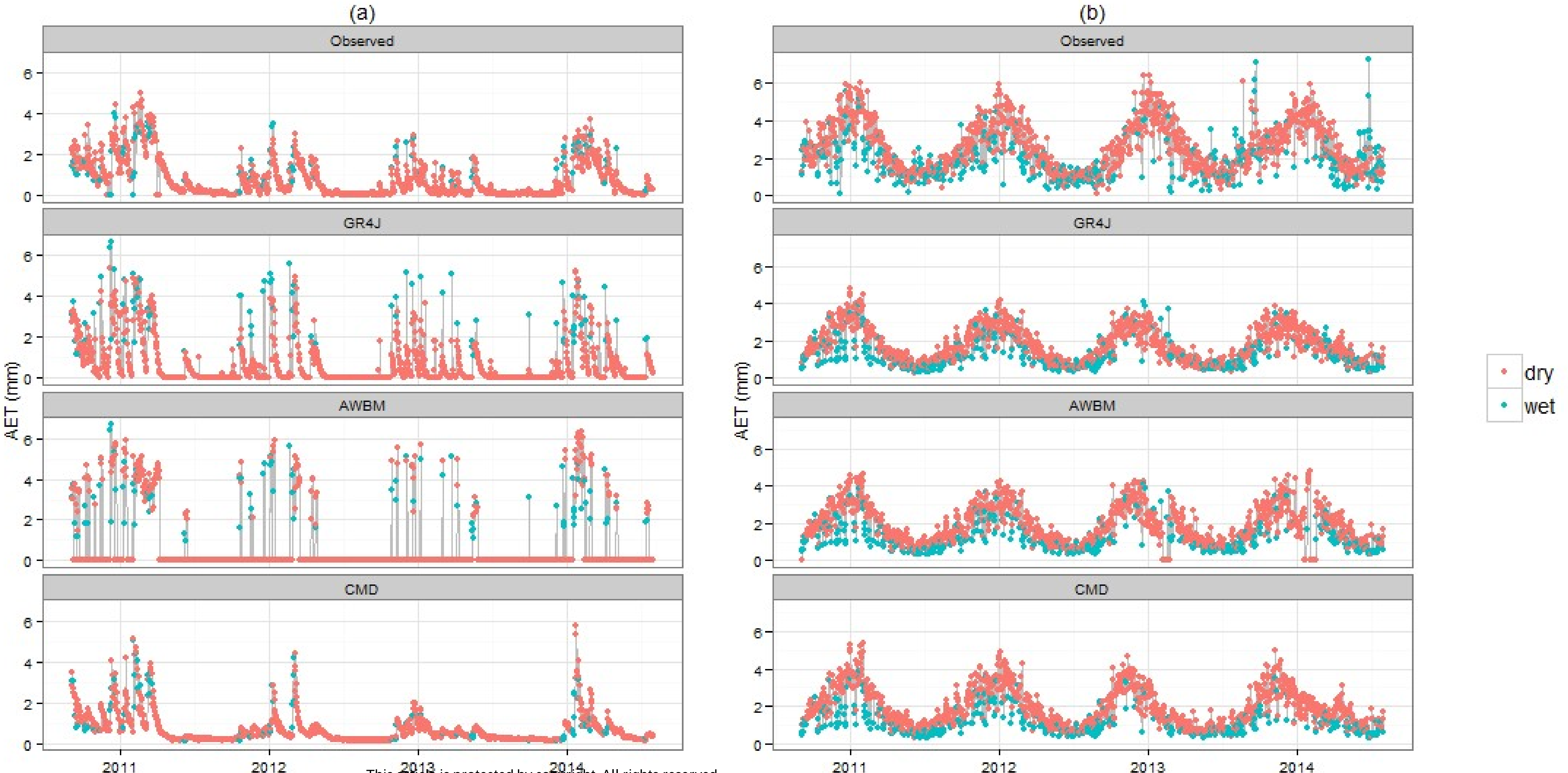
(a)
(b)
Observed
GR4J
AWBM
CMD
AET (mm)
0
2
4
6
2011
2012
2013
2014
dry
wet